

Response to editor

Dear Prof. Willy Maenhaut,

Thank very much for your help and edition.

Best regards,

Xiaohong

Prof. Xiaohong Yao (Ph.D)

Ocean University of China

Tracer-based investigation of organic aerosols in marine atmospheres from marginal seas of China to the northwest Pacific Ocean

Tianfeng Guo, Zhigang Guo, Juntao Wang, Jialiang Feng, Huiwang Gao, and Xiaohong Yao

For the Main text:

Lines 56-57: Replace "estimated the contribution of marine isoprene-derived SOA to the OC in marine atmospheric particles ranged from <0.2% on a global scale, but to as high as 50% (sub-micron OC) over the vast" by "estimated that the contribution of marine isoprene-derived SOA to the OC in marine atmospheric particles is <0.2% on a global scale, but that the hourly-averaged sub-micron OC emission may approach 50% over vast".

Line 108: Replace "analyzed in" by "measured in".

Line 132: Replace "were analyzed" by "were measured".

Response: We have corrected these accordingly.

For the Supplement:

Page 2, line 1: Replace "analyzed in" by "measured in".

Page 2, line 11: Replace "were analyzed" by "were measured".

Page 2, line 14: Replace "was analyzed" by "was measured".

Response: We have corrected these accordingly.

Furthermore, I noticed that your figures 1, 2, and 3 contain maps. To clarify the copyright, we differentiate between (a) maps entirely created by you, (b) maps created by you but based on layers reused from other originators, or (c) maps simply reused from other originators.

An example for (a) is a digital elevation model (DEM) purely based on measurement points collected by you and derived by using a software product. If you use an existing map layer from another originator as a basis for significantly enriching the map with your own content, this would be an example for case (b). Case (c) could be a pure reproduction of Google Maps where your own contribution is rather small (e.g. a city map where you only added a few marks for your study locations).

If the map was entirely created by you (case a), there is no need to change the caption or figure. However, if the map was not entirely created by you (cases b or c), please provide a new file in which the copyright is denoted in the figure itself. If this is not possible, please provide it in the caption.

Please make sure that the figure or caption contains the appropriate copyright statement as this is the responsibility of the authors.

Please let us know which case (a, b, or c) corresponds to the map used in your manuscript. Cases (b) and (c) need a copyright statement which consists of the copyright symbol © and the copyright holder (e.g. © Microsoft).

Response: Thanks. The maps in figure 1, 2, 3 in this manuscript correspond to case b. And the copyright statement has been added both in the figures and the figure captions as shown below.

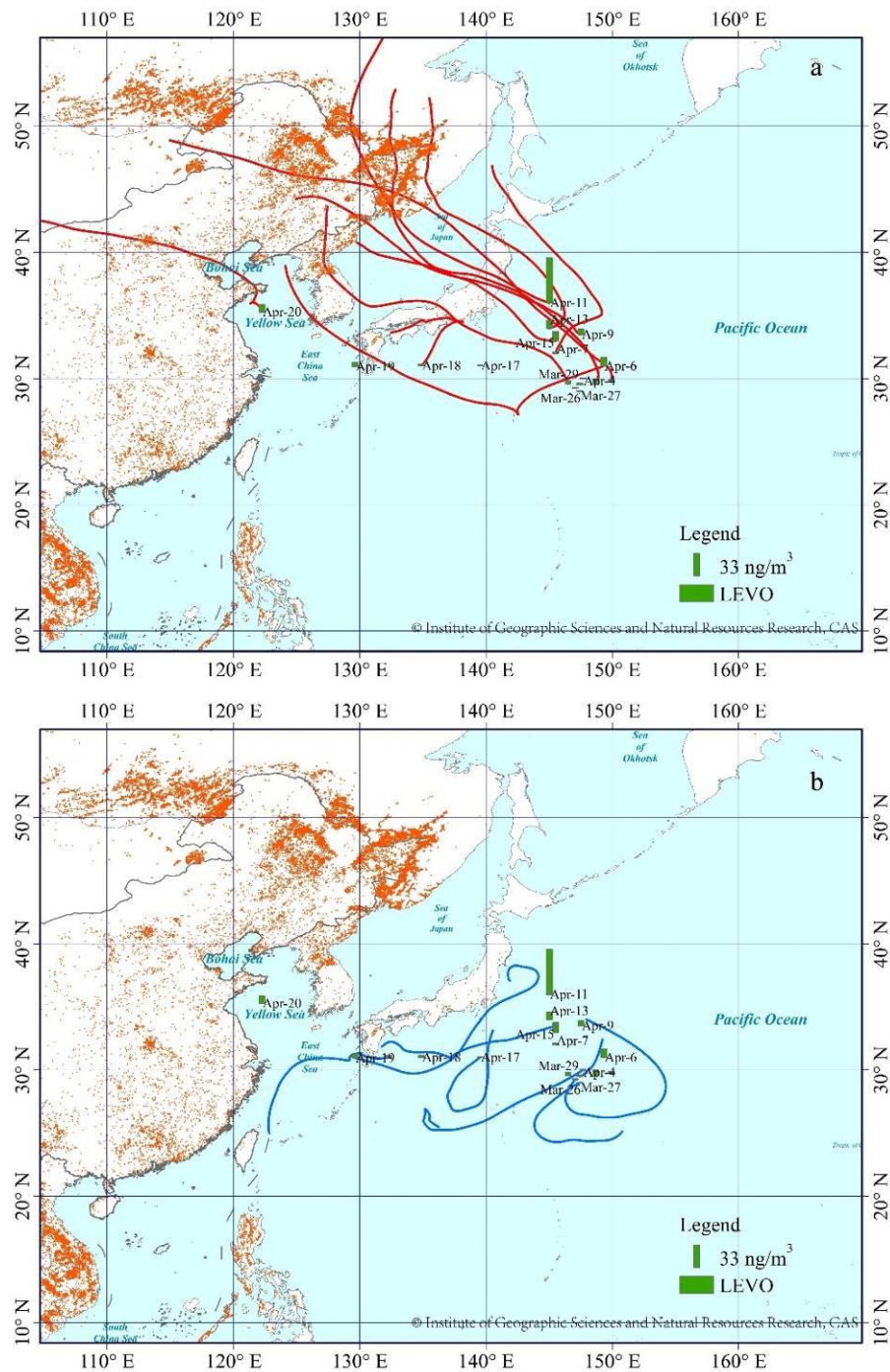


Figure 1. Spatial distribution of LEVO in TSP over the NWPO in spring of 2014 and 72-hrs back trajectory associated with each TSP sample. The red lines represent that air masses can be derived from the continent (a, Category 1); the blue lines represent that air masses may be derived mainly from the oceans (b, Category 2). The red dots represent the locations of fires from Fire Information for Resource Management System (FIRMS, <https://firms.modaps.eosdis.nasa.gov/>). And the base map was from Resource and Environment Data Cloud Platform (<http://www.resdc.cn/DOI>), DOI: 10.12078/2018110201, © Institute of Geographic Sciences and Natural Resources Research, Chinese Academy of Sciences (CAS). The data from Resource and Environment Data Cloud Platform are open and free.

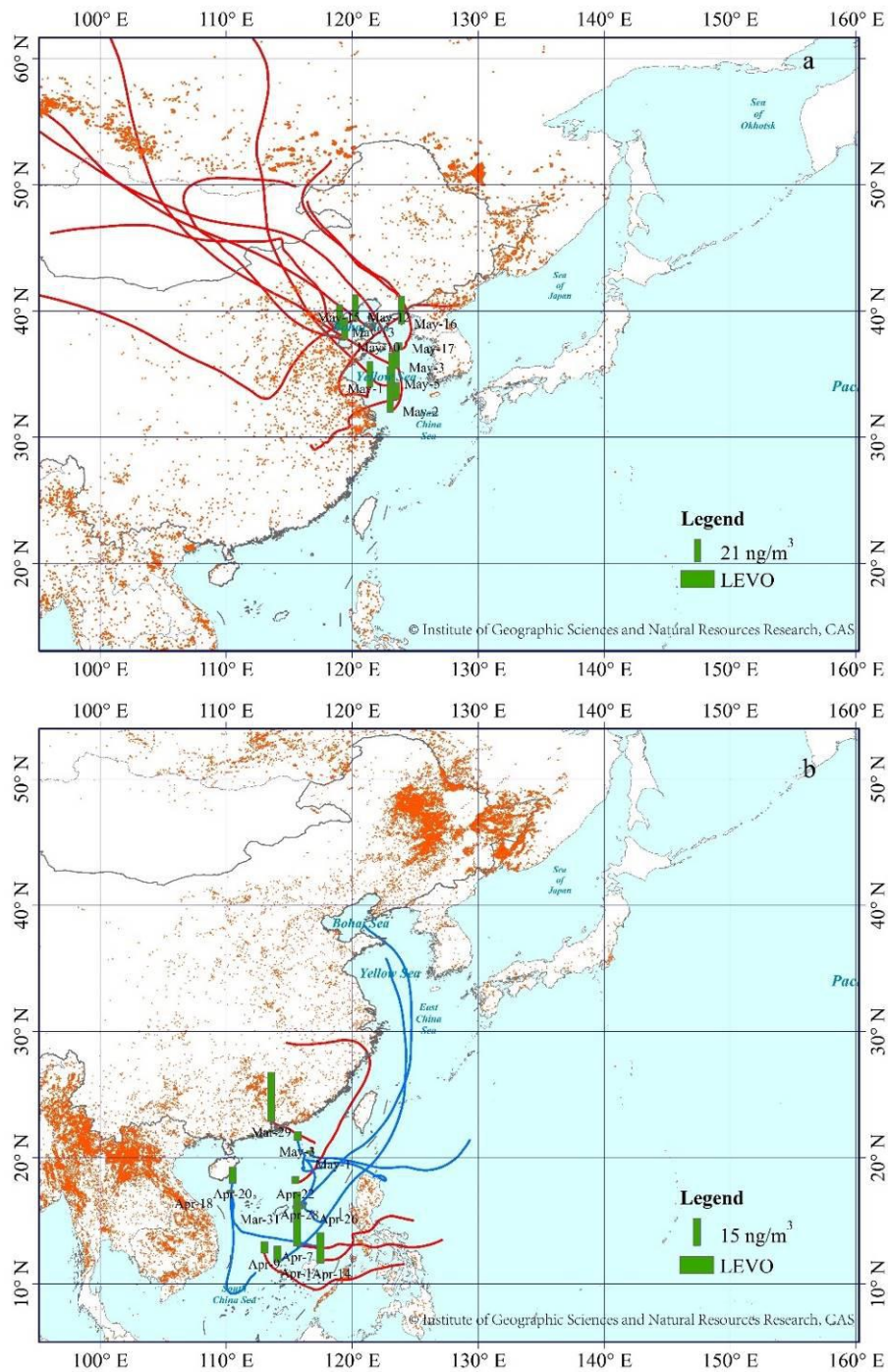


Figure 2. Spatial distribution of LEVO over the YBS (a, 2014), and SCS (b, 2017), detailed information described in Figure 1. And the base map was from Resource and Environment Data Cloud Platform (<http://www.resdc.cn/DOI>), DOI: 10.12078/2018110201, © Institute of Geographic Sciences and Natural Resources Research, Chinese Academy of Sciences (CAS).

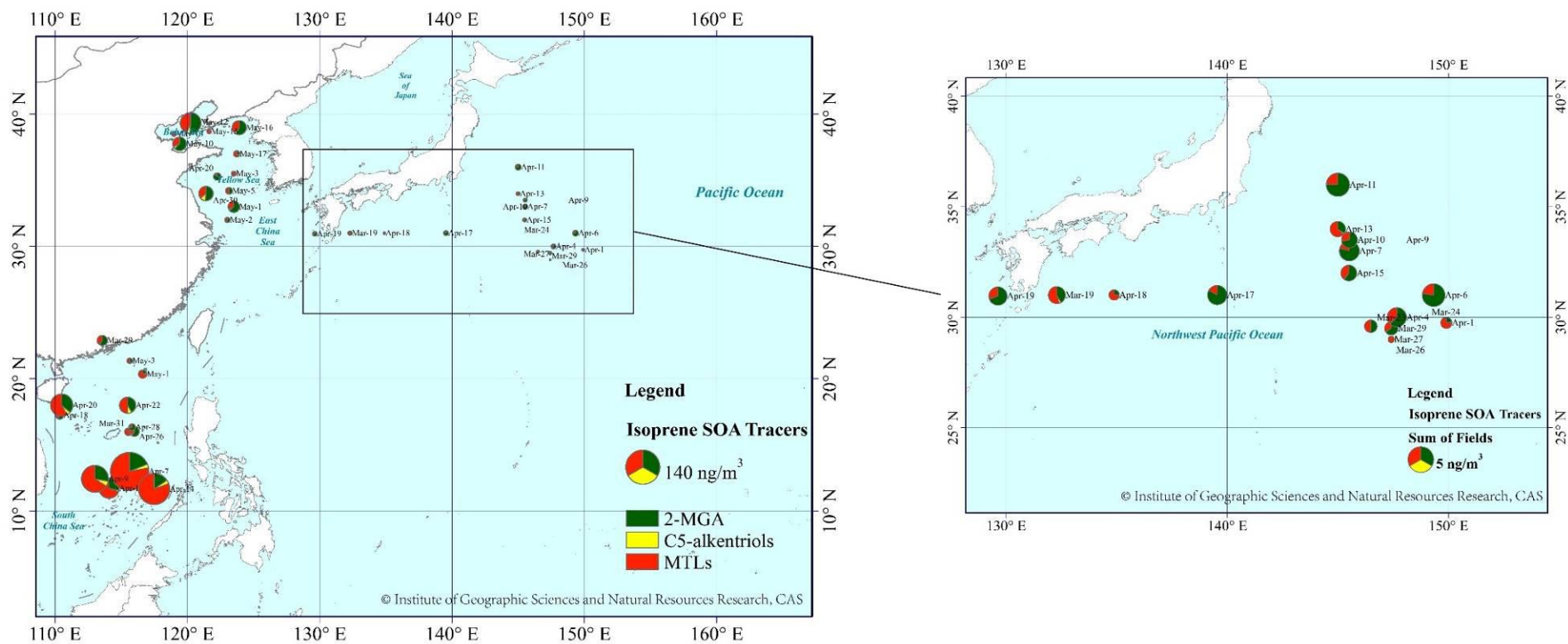


Figure 3. Spatial distribution of SOA_I tracer compounds over three marine regions, YBS and NWPO in 2014, SCS in 2017. The area of the pie indicates the concentration of total SOA_I tracers. And the base map was from Resource and Environment Data Cloud Platform (<http://www.resdc.cn/DOI>), DOI: 10.12078/2018110201, © Institute of Geographic Sciences and Natural Resources Research, Chinese Academy of Sciences (CAS).

Tracer-based investigation of organic aerosols in marine atmospheres from marginal seas of China to the northwest Pacific Ocean

Tianfeng Guo¹, Zhigang Guo¹, Juntao Wang², Jialiang Feng^{3*}, Huiwang Gao^{2,4}, Xiaohong Yao^{2,4*}

¹ Shanghai Key Laboratory of Atmospheric Particle Pollution and Prevention, Department of Environmental Science and Engineering, Fudan University, Shanghai 200433, China;

² Lab of Marine Environmental Science and Ecology, Ministry of Education, Ocean University of China, Qingdao 266100, China

³ School of Environmental and Chemical Engineering, Shanghai University, Shanghai 200444, China

⁴ Pilot National Laboratory for Marine Science and Technology (Qingdao), Qingdao, China

Correspondence to: Xiaohong Yao (xhyao@ouc.edu.cn); Jialiang Feng (fengjialiang@shu.edu.cn)

Abstract. We investigated the geographic distributions of organic tracers in total suspended particles over marginal seas of China, including the Yellow and Bohai seas (YBS) and the South China Sea (SCS), and the northwest Pacific Ocean (NWPO) in spring, when Asian outflows strongly affect downwind marine atmospheres. The comparison of levoglucosan observed in this study with values from the literature showed that the concentrations of biomass burning aerosols over the NWPO increased largely in 2014. More observations together with our snapshot measurement, however, need to confirm whether the large increase occurred continuously through the last decades. The increase led to a mean value of levoglucosan (8.2 ± 14 ng/m³) observed over the NWPO close to that over the SCS (9.6 ± 8.6 ng/m³) and almost half of that over the YBS (21 ± 11 ng/m³). Small geographic differences in monoterpene-derived and sesquiterpene-derived secondary organic tracer concentrations were obtained among the three atmospheres, although the causes may differ. By contrast, a large difference in isoprene-derived secondary organic tracer concentrations was observed among the three atmospheres, with the sum of tracer concentrations over the SCS (45 ± 54 ng/m³) several times and approximately one order of magnitude greater than that over the YBS (15 ± 16 ng/m³) and the NWPO (2.3 ± 1.6 ng/m³), respectively. The geographic distribution of aromatic-derived secondary organic tracers was similar to that of isoprene-derived secondary organic tracers, with a slightly narrower difference, i.e., 1.8 ± 1.7 ng/m³, 1.1 ± 1.4 ng/m³ and 0.3 ± 0.5 ng/m³ over the SCS, the YBS and the NWPO, respectively. We discuss the causes of the distinctive geographic distributions of these tracers and present the tracer-based estimation of organic carbon.

1 Introduction

Aerosols that emanate from biomass burning (BB) consist primarily of carbonaceous components and inorganic salts, which can affect the climate directly by absorbing solar radiation or indirectly by acting as either cloud condensation nuclei (CCN) or ice nuclei (IN) (Bougiatioti et al., 2016; Chen et al., 2017; Hsiao et al., 2016). High BB aerosol emissions zones include boreal forests (e.g., in Eurasia and North America), tropical forests (e.g., in southeast Asia and the tropical Americas), and agriculture areas where crop residuals are burned (e.g., in developing countries such as China and India, etc.) (van der Werf et al., 2006). BB aerosols can undergo

39 long-range transport in the atmosphere, which can carry them from the continents to the oceans (Ding et al.,
40 2013; Fu et al., 2011; Kanakidou et al., 2005). For example, BB aerosols from boreal forest wildfires in Russia
41 and China reportedly made an appreciable contribution to atmospheric particle loads observed over the Arctic
42 Ocean and northwestern Pacific Ocean (NWPO) based on specific tracers of BB (Ding et al., 2013). Although
43 open wildfires from forests occur sporadically in terms of strength and occurrence frequency, global warming
44 could be conducive to vegetation fires (Running, 2006) and thus increase emissions of BB aerosols. In this
45 century, nine years were among the ten hottest global years on record, with 2014–2018 being ranked as the top
46 five hottest years (<https://www.climatecentral.org/gallery/graphics/the-10-hottest-global-years-on-record>). The
47 question is automatically raised: how do BB aerosols in the marine atmosphere in the hottest global years
48 change against those observations previously reported?

49 In addition to BB aerosols, secondary oxidation of biogenic volatile organic compounds (BVOCs) and
50 anthropogenic VOCs (AVOCs) also contribute to the particulate carbonaceous components of marine
51 atmospheres (Kanakidou et al., 2005). Secondary organic aerosols (SOAs) arising from the oxidation of
52 phytoplankton-derived isoprene have been argued to affect the chemical composition of marine atmospheric
53 aerosols and consequently impact CCN loading and cloud droplet number concentrations (Ekström et al., 2009;
54 Meskhidze and Nenes, 2006), but the importance of the marine isoprene-derived SOA is still debated (Arnold et
55 al., 2009; Claeys et al., 2010; Gantt et al., 2009; Guenther et al., 1995). For example, Gantt et al. (2009)
56 ~~estimated the contribution of marine isoprene-derived SOA to the OC in marine atmospheric particles ranged~~
57 ~~from <0.2% on a global scale, but to as high as 50% (sub-micron OC) over the vast~~ **estimated that the**
58 **contribution of marine isoprene-derived SOA to the OC in marine atmospheric particles is <0.2% on a global**
59 **scale, but that the hourly-averaged sub-micron OC emission may approach 50% over vast** regions of the oceans
60 during the midday hours when isoprene emissions are highest. Several modeling studies have shown that the
61 NWPO may experience the greatest increases in sea surface temperature and CO₂ input under a future warming
62 climate (John et al., 2015; Lauvset et al., 2017). The Kuroshio Extension current system leads the NWPO to be
63 an active subtropical cyclone basin, promoting biogenic activities (Hu et al., 2018). From the perspective of
64 global change, it is a long-term need to study the dynamic changes in atmospheric aerosols derived from marine
65 sources over the NWPO and adjacent marginal seas of China, as well as their potential effects on climate.

66 More importantly, BVOCs emitted from continental ecosystems and their oxidation products can significantly
67 affect the atmosphere in remote marine areas through long-range transport (Ding et al., 2013; Fu et al., 2011; Hu
68 et al., 2013a; Kang et al., 2018; Kawamura et al., 2017). BVOCs consist primarily of isoprene, monoterpenes,
69 sesquiterpenes, and their oxygenated hydrocarbons such as alcohols, aldehydes, and ketones (Ehn et al., 2014;
70 Guenther et al., 2006) and account for the majority of the global VOC inventory (Heald et al., 2008; Zhu et al.,
71 2016a, b). However, emission fluxes and oxidation processes of BVOCs show great variation, depending on
72 global warming and other factors such as regional landscape, other pollutants in the ambient air, etc. (Ait-Helal
73 et al., 2014; Claeys et al., 2004; Hu and Yu, 2013; Peñuelas and Staudt, 2010). Unlike a potential increase in
74 BVOC-derived organics aerosols in marine atmospheres under global warming, anthropogenic VOCs and
75 carbonaceous particles over the continents have been decreased because of effective mitigation of air pollutants
76 in the last decades (Li et al., 2019; Murphy et al., 2011; Sharma et al., 2004; Zhang et al., 2012). In the northern
77 hemisphere, marine atmospheres are also usually affected by anthropogenic pollutants to some extent, most of
78 which are derived from long-range transport from continents (Bao et al., 2018; Kang et al., 2019; Zhang et al.,
79 2017). The reverse trends in BVOC and anthropogenic VOC would change the composition, sources of
80 carbonaceous particles in marine atmospheres. Updated observations are thereby needed to reveal the change
81 and service the future study of the impacts.

82 In this study, we determined the concentrations of some typical organic tracers in aerosol samples obtained from

83 three cruise campaigns from the marginal seas of China, including in the South China Sea (SCS) in 2017,
84 Yellow Sea and Bohai Sea (YBS), to the NWPO in 2014, both in springtime. We investigated the influences of
85 BB aerosols from continents over three marine atmospheres, quantified the contributions of various precursors
86 to the observed SOA in marine atmospheres using organic tracers established in the literature, and explored the
87 formation pathways of SOA from their precursors during long-range transport in these hottest global years.
88 Particularly, we conducted a comprehensive comparison of this observation with those reported in literature in
89 terms of long-term variations and geographic distributions of these tracers, etc.

90 **2 Materials and Methods**

91 Total suspended particulate (TSP) samples were collected over the NWPO from 19 March to 21 April 2014,
92 over the YBS from 30 April to 17 May 2014, and over the SCS from 29 March to 4 May 2017. All samples were
93 collected on the upper deck of the R/V Dong Fang Hong II, which sits ~8 m above the sea surface. To avoid
94 contamination from the ship's exhaust, samples were collected only when the ship was sailing, and the wind
95 direction ranged from -90° to 90° relative to the bow. TSP samples were collected on quartz fiber filters
96 (Whatman QM-A) that had been pre-baked for 4 h at 500°C prior to sampling using a high-volume sampler
97 (KC-1000, Qingdao Laoshan Electric Inc., China). The sampling duration was 15–20 h at a flow rate of ~ 1000 L
98 /min. After sampling, the sample filters were wrapped in baked aluminum foil and sealed in polyethylene bags,
99 then stored at -20°C and transported to the laboratory. Field blanks were collected during each sampling period.
100 However, one sampler was out of service during the cruise on the SCS. As a compromise, cellulose filters
101 (Whatman 41) previously intended for elemental analyses were used for analyses of the organic tracers in TSP.
102 The method for determining the concentrations of tracers was adapted from Kleindienst et al. (2007) and Feng et
103 al. (2013). Briefly, 20 mL dichloromethane/methanol (1:1, v/v) was used for ultrasonic extraction of 40 cm^2 of
104 each filter at room temperature three times. The combined extracts were filtered, dried under a gentle stream of
105 ultrapure nitrogen, and then derivatized with 100 μL N,O-bis-(trimethylsilyl)-trifluoroacetamide (BSTFA,
106 containing 1% trimethylchlorosilane as a catalyst) and 20 μL pyridine at 75°C for 45 min. Gas chromatography
107 mass spectrometry (GC-MS) analyses were conducted with an Agilent 6890 GC/5975 MSD. Prior to solvent
108 extraction, methyl- β -D-xylanopyranoside (MXP) was spiked into the samples as an internal/recovery standard.
109 Hexamethylbenzene was added prior to injection as an internal standard to check the recovery of the surrogates.
110 Like those reported by Feng et al. (2013), the primary organic tracers ~~analyzed in~~ **measured in** this study
111 included levoglucosan (LEVO), mannosan, and galactosan. Four types of secondary organic tracers were used:
112 isoprene-derived secondary organic tracers (SOA_I) including 2-methylglyceric acid (2-MGA), C5-alkene triols
113 (cis-2-methyl-1,3,4-trihydroxy-1-butene, 3-methyl-2,3,4-trihydroxy-1-butene and
114 trans-2-methyl-1,3,4-trihydroxy-1-butene), and MTLs (2-methylthreitol and 2-methylerythritol);
115 monoterpene-derived secondary organic tracers (SOA_M) including 3-hydroxyglutaric acid (HGA),
116 3-hydroxy-4,4-dimethylglutaric acid (HDMGA), and 3-methyl-1,2,3-butanetricarboxylic acid (MTBCA); the
117 sesquiterpene-derived secondary organic tracer (SOA_S) β -caryophyllinic acid; and the aromatic
118 (toluene)-derived secondary organic tracer (SOA_A) 2,3-dihydroxy-4-oxopentanoic acid (DHOPA). LEVO was
119 quantified based on authentic standards in this study. While the SOA tracers without available commercial
120 standards were quantified using methyl- β -D-xylanopyranoside (MXP) as a surrogate. To reduce the uncertainty
121 of quantification, relative response factors of the target tracers to MXP were estimated by comparing the area
122 ratio of typical target ions to MXP to that of total ions in selected samples that showed high concentrations of
123 the target tracers (Feng et al., 2013).
124 Field blanks and laboratory blanks (ran every 10 samples) were extracted and analyzed in the same manner as
125 the ambient samples. Target compounds were nearly always below the detection limit in field and laboratory

126 blanks. Recoveries of the surrogate (MXP) were in the range of 70–110%. The reported results were corrected
127 for recovery, assuming that the target compounds had the same recovery as the surrogate. Duplicate analyses
128 indicated that the deviation was less than 15%.

129 However, the substitution of cellulose filters (Whatman 41) during the cruise on the SCS led to increased field
130 blank values for some tracers. The tracer concentrations in those samples were, however, over three times higher
131 than the field blank values, except for those of mannosan and galactosan. Data for mannosan and galactosan
132 were thus not available, nor were the total organic carbon concentrations, for samples collected during the cruise
133 on the SCS.

134 The concentrations of organic carbon (OC) and element carbon (EC) in each sample ~~were analyzed~~ were
135 **measured** with a DRI 2001A thermal/optical carbon analyzer (Atmoslytic Inc., Calabasas, CA, USA) using the
136 IMPROVE temperature program (Wang et al., 2015). All filters before and after sampling were weighted at a
137 glovebox under controlled ambient temperature and relative humidity. Mass concentrations of TSP, however,
138 should be treated as semi-quantitative results by considering analytic errors of quartz fiber filters (Yao et al.,
139 2009).

140 3. Results and Discussion

141 3.1 Spatiotemporal distributions of LEVO

142 Levoglucosan, mannosan, and galactosan produced by the pyrolysis of cellulose and hemicellulose have been
143 widely used as organic tracers of BB aerosols in ambient air (Ding et al., 2013; Fu et al., 2011; Feng et al.,
144 2013). The mean levels of LEVO in TSP collected during the cruises on the NWPO and the SCS were
145 comparable, at 8.2 ng/m³ and 9.6 ng/m³, respectively (Figure S1, Table 1). They were almost half of the mean
146 value of 21 ng/m³ during the cruise on the YBS, where high concentrations of BB aerosols have been observed
147 in continental atmospheres upwind of the YBS mainly from wildfires and the burning of crop residue, wildfire,
148 etc. (Feng et al., 2012; Feng et al., 2013; Yang et al., 2014). Unlike the small difference among the mean values,
149 the concentration of LEVO fluctuated greatly among TSP samples in each oceanic zone, ranging from 0.5 to 65
150 ng/m³ over the NWPO, from 1.0 to 30 ng/m³ over the SCS and from 2.5 to 42 ng/m³ over the YBS (Fig. S1).
151 High spatiotemporal variation in LEVO in TSP has also been observed in literature, with concentrations of
152 LEVO fluctuating around 0.2–41 ng/m³ during Arctic to Antarctic cruises from July to September 2008 and
153 from November 2009 to April 2010 (Hu et al., 2013b). Hu et al. (2013b) also reported the highest LEVO
154 concentrations occurring at mid-latitudes (30°–60° N and S) and the lowest at Antarctic and equatorial latitudes
155 over the several months of sampling. This distinctive geographical distribution was not observed in the present
156 study, as there were no significant differences in LEVO in TSP between the SCS and NWPO ($P > 0.05$).

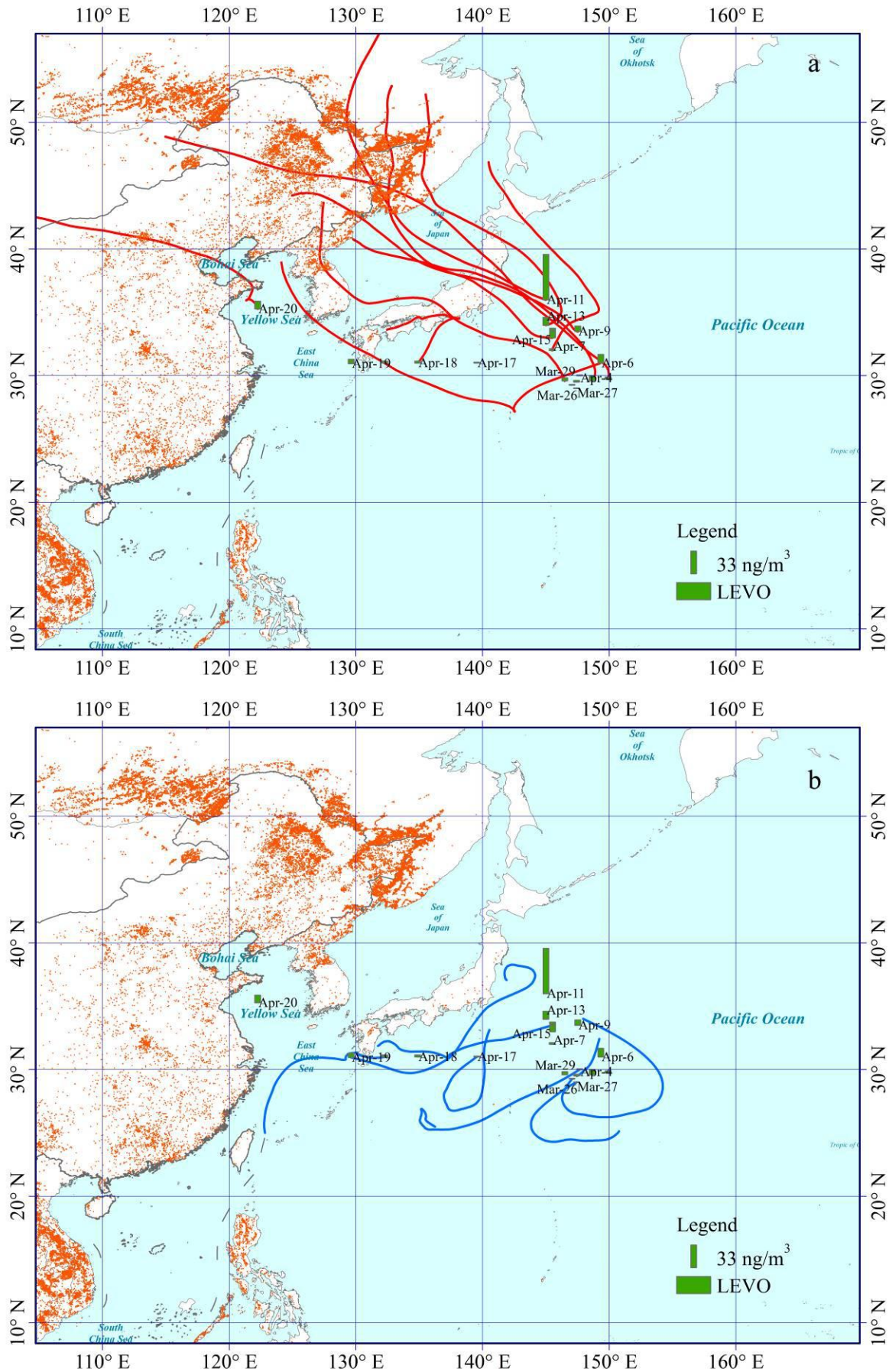
157 Narrow spatiotemporal variation in LEVO in TSP has been reported during summer sampling over the North
158 Pacific Ocean and the Arctic in 2003, with maximum and mean values as low as 2.1 ng/m³ and 0.5 ng/m³,
159 respectively (Ding et al., 2013). A lower mean value of LEVO of 1.0 ng/m³ has also been reported in the spring
160 over the island of Chichi-jima from 2001 to 2004 (Mochida et al., 2010), while the levels increased to 3.1 ± 3.7
161 ng/m³ in TSP collected on the island of Okinawa in 2009–2012 (Zhu et al., 2015). Using these previous
162 observations as a reference (Table 1), our observations suggest that the BB aerosols from the long-range
163 transport over the NWPO in 2014 largely increased. Thus, an important question is raised, i.e., does the increase
164 occur continuously and largely over the last decades in marine atmospheres over the NWPO? Due to the lack of
165 BB sources in oceans, large spatiotemporal variation in the concentrations of LEVO in the marine atmosphere
166 may be related to the long-range transport of atmospheric particles from continents. Thus, 72 h back trajectories

167 of air masses at a height of 1000 m during our sampling periods (Figs. 1, 2) were calculated using the HYSPLIT
168 model (<https://ready.arl.noaa.gov/HYSPLIT>). Based on the calculated back trajectories, TSP samples could be
169 classified into two categories with Category 1 representing continent-derived aerosol samples and Category 2
170 being ocean-derived aerosol samples. All 12 samples collected over the YBS fell into Category 1 (Fig. 2). Half
171 (11/19) of the samples collected over the NWPO were classified into Category 1 (Fig. 1). A significant
172 difference ($p < 0.05$) was obtained between the concentrations of LEVO in Category 1 ($13 \pm 18 \text{ ng/m}^3$) and
173 Category 2 ($2.0 \pm 1.8 \text{ ng/m}^3$) over the NWPO. The values in Category 2 were closer to the springtime
174 observations reported by Mochida et al. (2010) and Zhu et al. (2015) as well as the summer observations
175 reported by Ding et al. (2013), reflecting the marine background value less affected by continental air masses.
176 On the other hand, the much higher values in Category 1 than Category 2 further indicate a large increase in
177 contribution of BB aerosols being transported from the continents to the remote marine atmosphere in 2014.
178 On 11 April 2014 over the NWPO, an episode of high LEVO concentration of 65 ng/m^3 occurred (Fig. 1). Like
179 LEVO, the concentrations of galactosan and mannosan in the sample were also the highest among all samples
180 collected over the NWPO. This sample was collected in the oceanic zone, approximately 500 km from the
181 continent of Japan. A combination of air mass back trajectories and NASA's FIRMS Fire Map indicated strong
182 BB aerosol emissions from intense fire events in Siberia, followed by long-range transport with the westerly
183 wind as the major contributors to this anomaly (Fig. 1). A similar episodic concentration of LEVO of 27 ng/m^3
184 in TSP was observed once previously over the NWPO during a circumnavigation cruise (Fu et al., 2011). By
185 combining satellite data with other observations, many studies in literature have found that BB aerosols from
186 major forest fires and smoke events in Siberia could be transported downwind to remote marine regions not only
187 in spring, but also in summer (Ding et al., 2013; Generoso et al., 2007; Huang et al., 2009). In a few cases, BB
188 aerosols have been reported to have reached as far as the adjacent Arctic region (Generoso et al., 2007; Warneke
189 et al., 2010). Van der Werf et al. (2006) estimated the emissions of BB aerosols from Eurasia to be much larger
190 than those from North America. Thus, it is not surprising that the concentrations of LEVO over the NWPO were
191 much higher than those over the eastern North Pacific and western North Atlantic at similar latitudes (Hu et al.,
192 2013b).

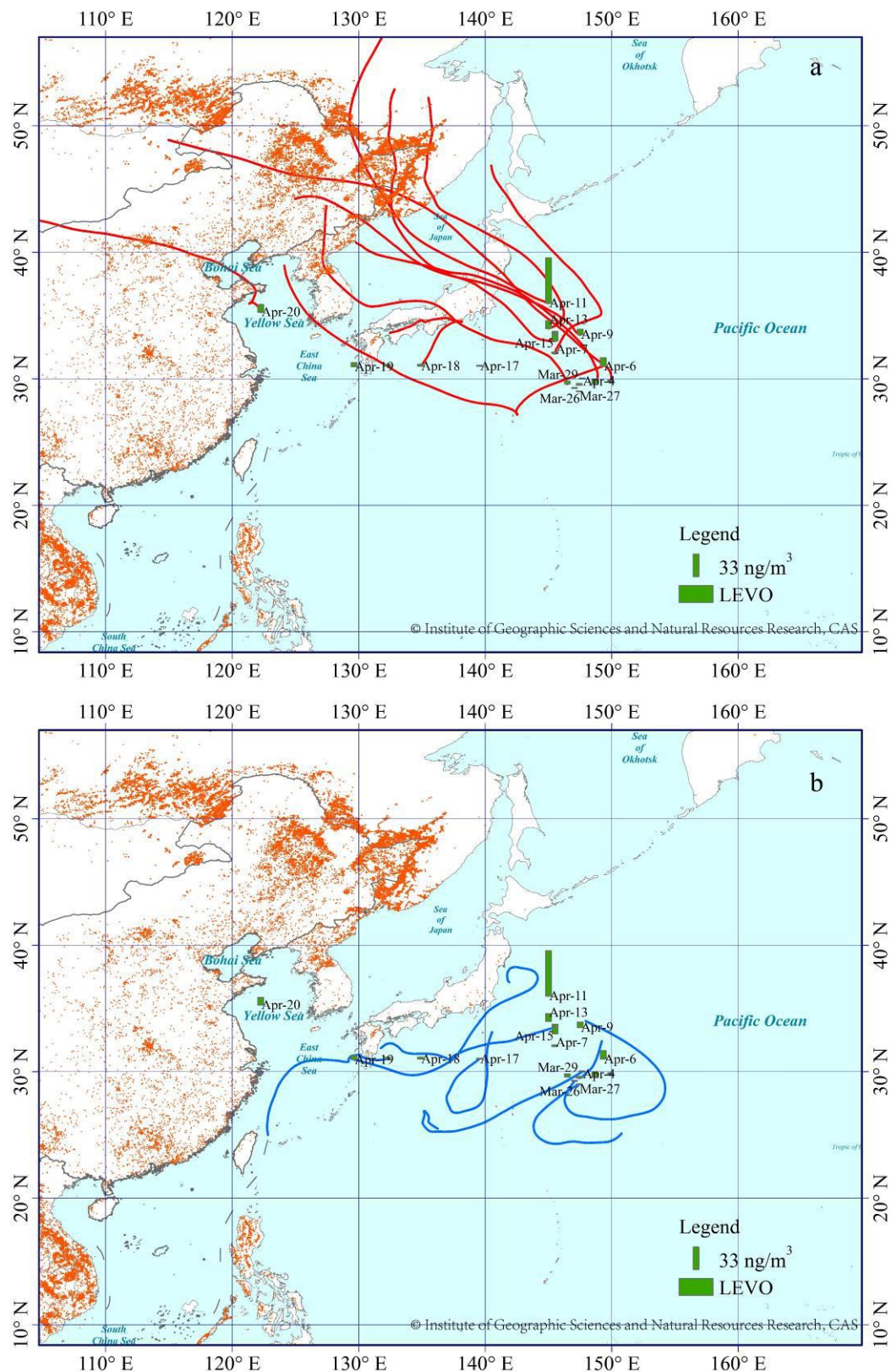
193 In addition, both galactosan and mannosan showed strong linear correlations with LEVO ($R^2 = 0.98$, $p < 0.05$)
194 in TSP collected over the NWPO and YBS in this study. These strong correlations indicate that the three tracers
195 were probably derived from the same BB sources. Previous studies have reported LEVO/mannosan (L/M) ratios
196 of 3–10, 15–25, and 25–40 from softwood, hardwood, and crop-residue burning, respectively (Kang et al., 2018;
197 Zhu et al., 2015). The calculated L/M ratios in TSP collected over the NWPO were 19 ± 4 in this study, which
198 implies dominant contributions from herbaceous plants and hardwood. The calculated L/M ratios in TSP
199 collected over the YBS were 14 ± 11 , indicating mixed sources.

200 In all, 5 of 13 samples collected over the SCS were classified into Category 1, with air masses identified as
201 originating from either the continental areas of South China or the Philippines (Fig. 2). The concentration of
202 LEVO fluctuated around $17 \pm 12 \text{ ng/m}^3$ in Category 1 but decreased to $3.6 \pm 3.4 \text{ ng/m}^3$ in Category 2. However, no
203 significant difference was found between categories due to the large variation in LEVO concentration among the
204 limited number of samples in Category 1 ($p > 0.05$). Forest fires occur accidentally, leading to the large variation
205 in LEVO in Category 1. Southern Asia has been reported to be one of the greatest emission sources of BB
206 aerosols worldwide (van der Werf et al., 2006), which likely led to the higher mean value of LEVO in Category
207 1. However, the LEVO level observed over the SCS in Category 2 was closer to that reported from low-latitude
208 regions ($2.7 \pm 1.1 \text{ ng/m}^3$, Table 1) collected during a global circumnavigation cruise (Hu et al., 2013b). Hu et al.
209 (2013b) argued that their low observed concentrations may have been associated with intense wet deposition,
210 degradation as well as intensive moist convection that occurred in the tropical region during their summer cruise.

211 Unfortunately, no previous observations of LEVO in spring can allow us analyzing the long-term variation in
 212 contribution of BB aerosols therein. However, this observation can be used for future comparison.

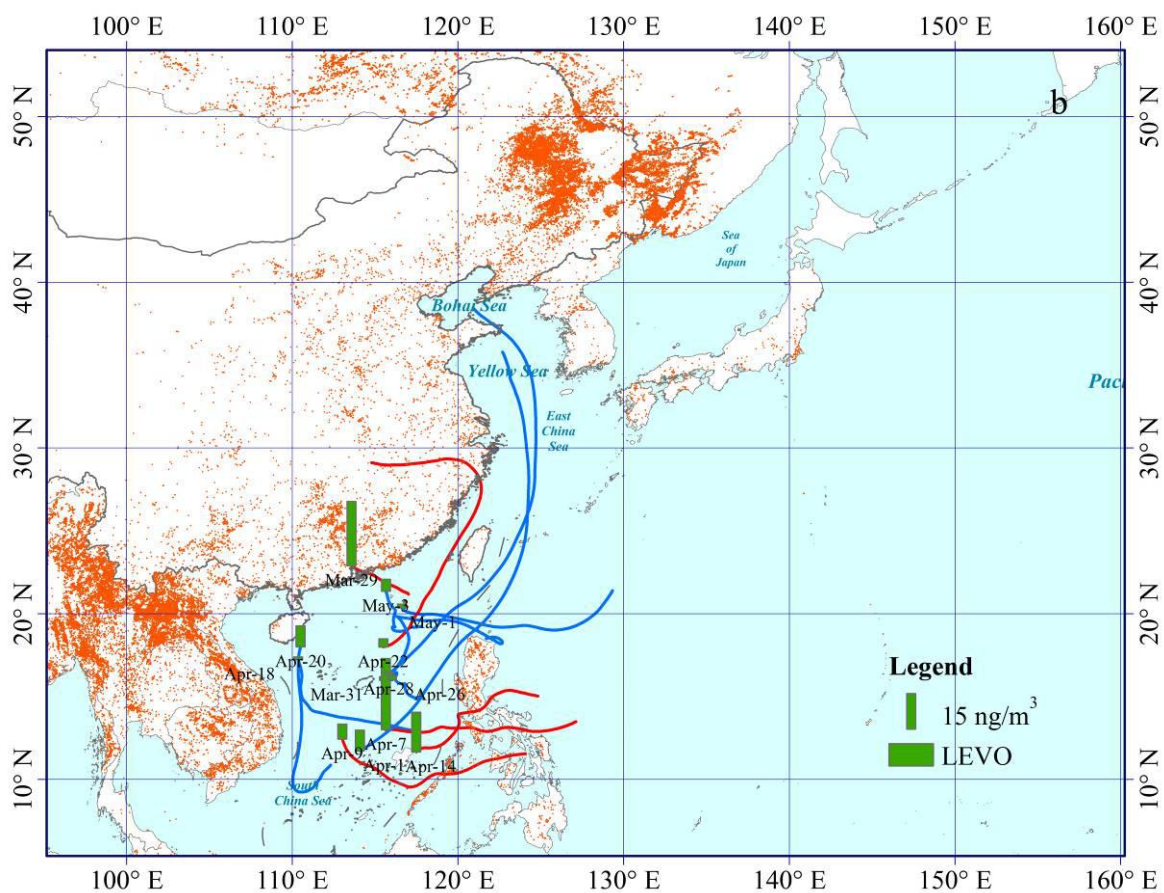
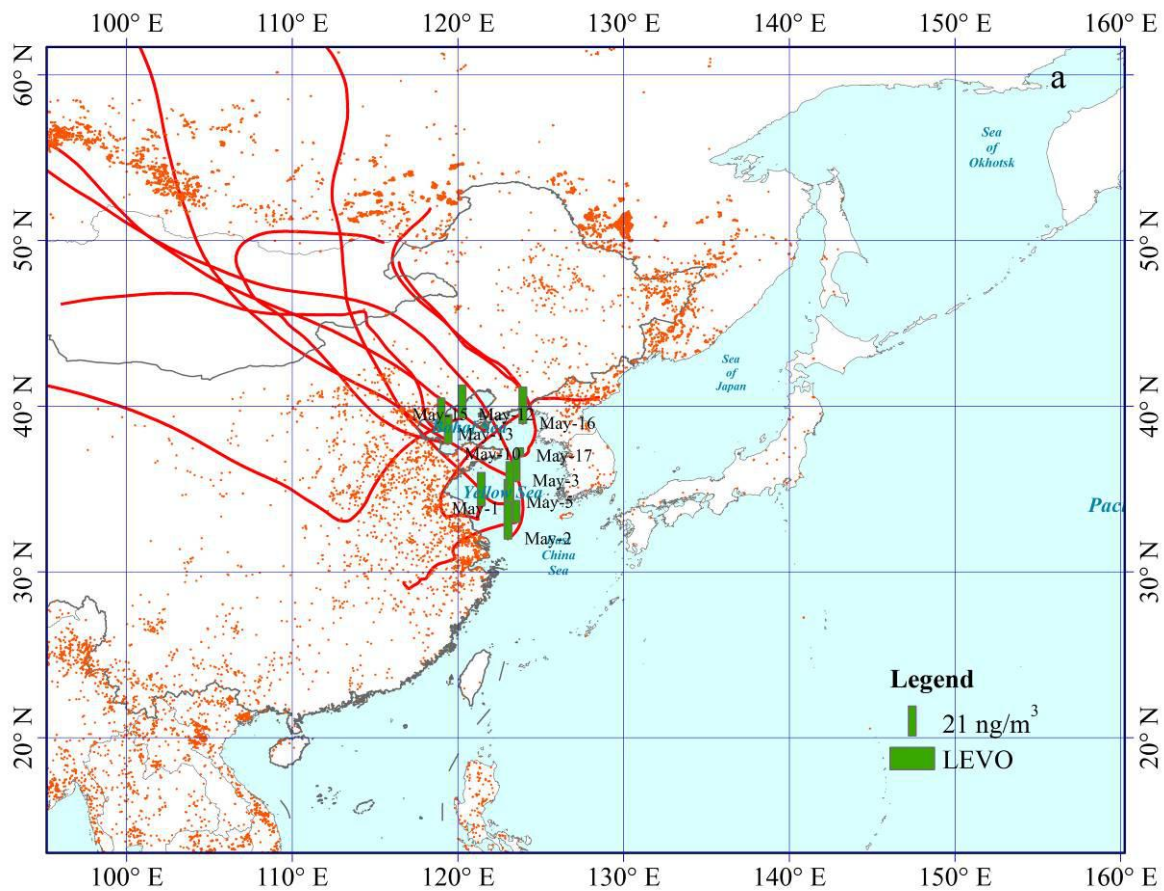


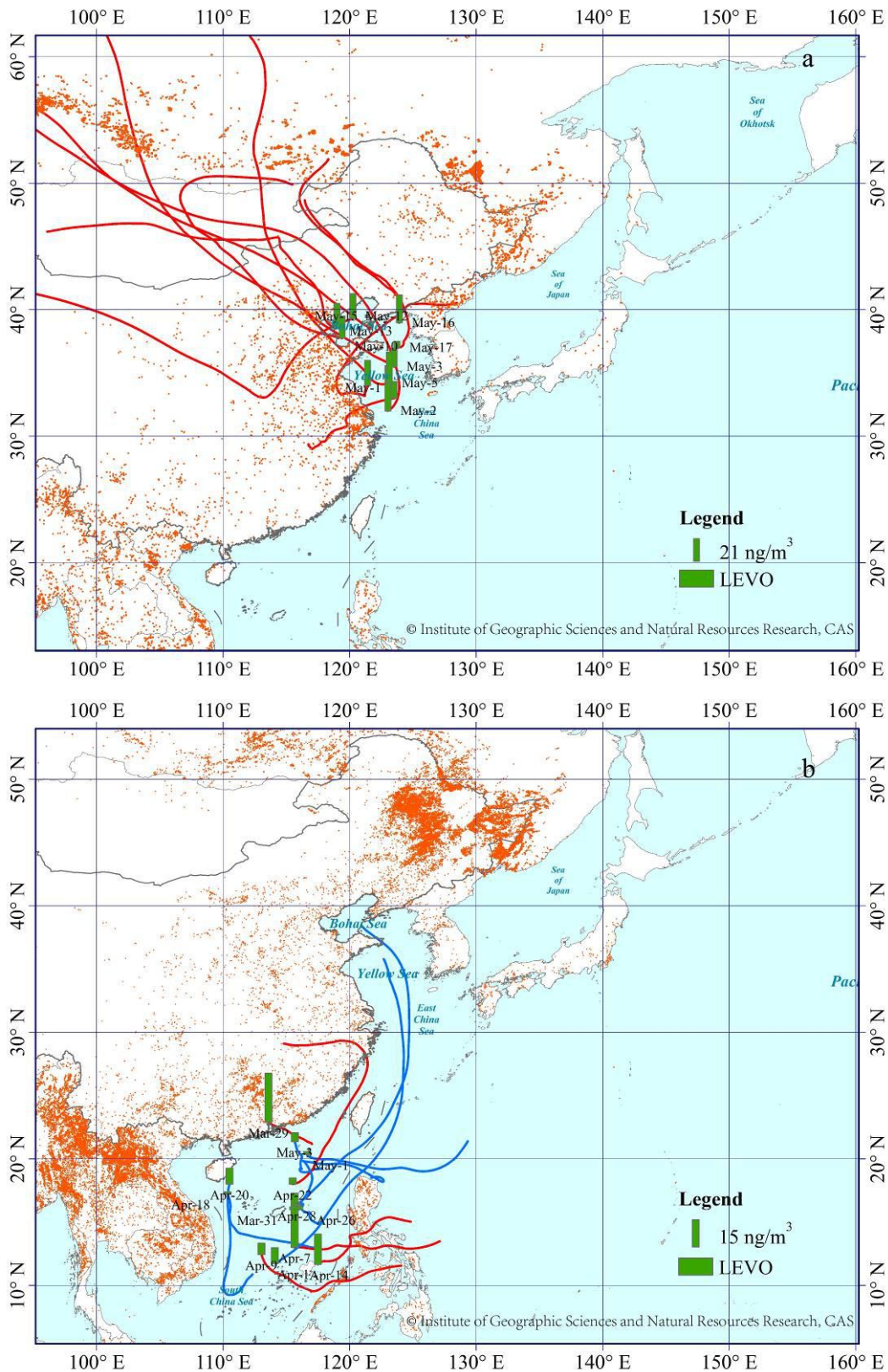
213



214

215 **Figure 1. Spatial distribution of LEVO in TSP over the NWPO in spring of 2014 and 72-hrs back**
 216 **trajectory associated with each TSP sample. The red lines represent that air masses can be derived from**
 217 **the continent (a, Category 1); the blue lines represent that air masses may be derived mainly from the**
 218 **oceans (b, Category 2). The red dots represent the locations of fires from Fire Information for Resource**
 219 **Management System (FIRMS, <https://firms.modaps.eosdis.nasa.gov/>).** And the base map was from
 220 **Resource and Environment Data Cloud Platform (<http://www.resdc.cn/DOI>), DOI: 10.12078/2018110201,**
 221 **[© Institute of Geographic Sciences and Natural Resources Research, Chinese Academy of Sciences \(CAS\).](http://www.resdc.cn/DOI)**
 222 **[The data from Resource and Environment Data Cloud Platform are open and free.](http://www.resdc.cn/DOI)**





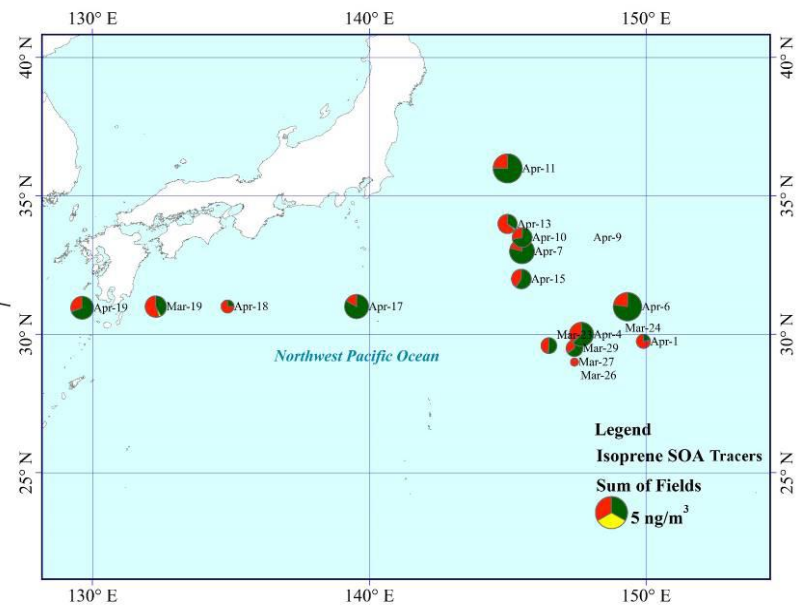
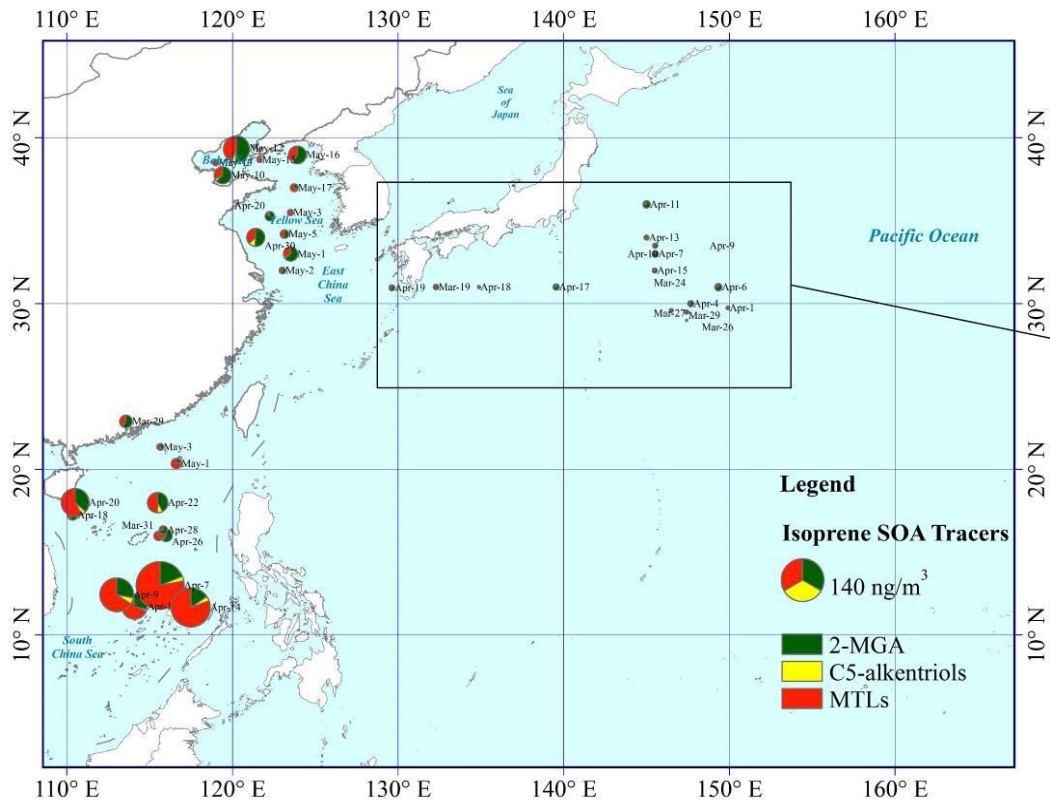
224

225 **Figure 2. Spatial distribution of LEVO over the YBS (a, 2014), and SCS (b, 2017), detailed information**
 226 **described in Figure 1. And the base map was from Resource and Environment Data Cloud Platform**
 227 **(<http://www.resdc.cn/DOI>), DOI: 10.12078/2018110201, © Institute of Geographic Sciences and Natural**
 228 **Resources Research, Chinese Academy of Sciences (CAS).And the base map was from Resource and**
 229 **Environment Data Cloud 210 Platform, DOI: 10.12078/2018110201.**

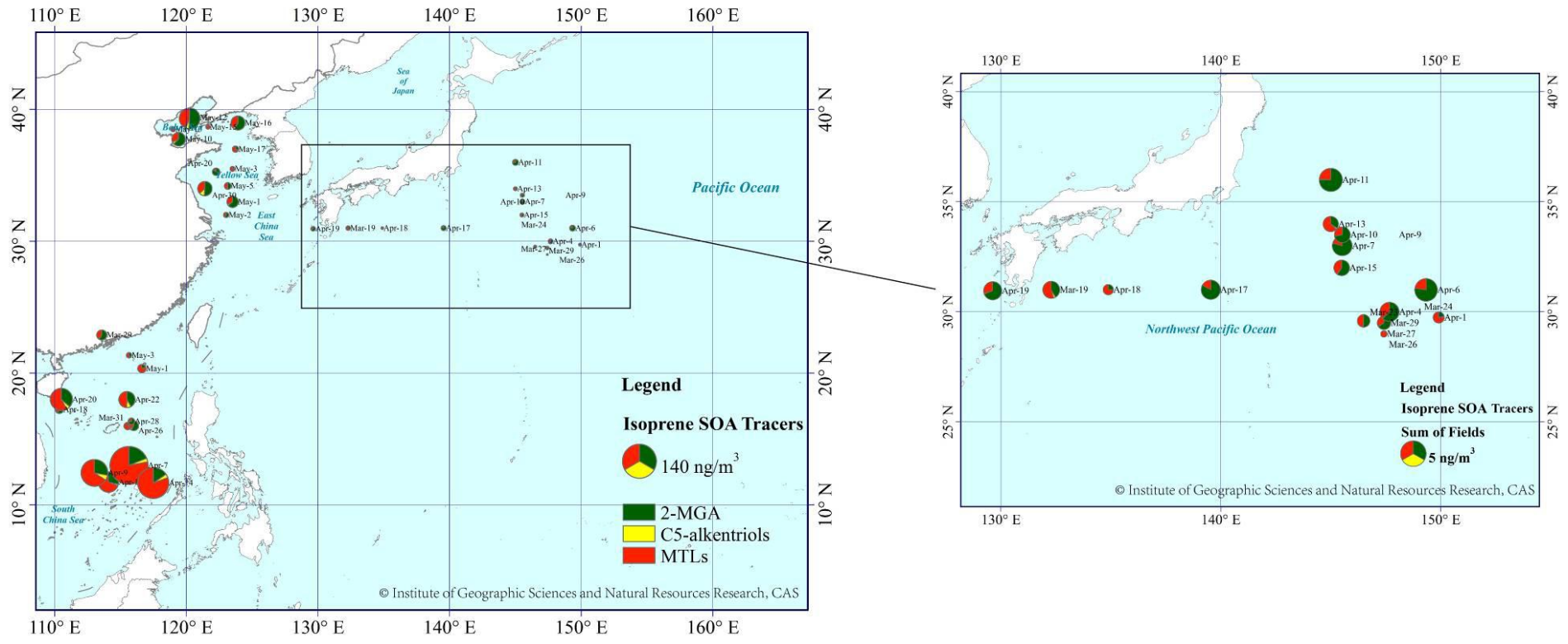
230 3.2 Spatiotemporal distributions of SOA_I tracers

231 SOA_I tracers were detected during all three cruises. The sum of SOA_I tracers showed a decreasing trend of up to
232 approximately one order of magnitude from marginal seas to the open ocean, i.e., $45 \pm 54 \text{ ng/m}^3$ in TSP over the
233 SCS, $15 \pm 16 \text{ ng/m}^3$ over the YBS and $2.3 \pm 1.6 \text{ ng/m}^3$ over the NWPO (Fig. S1). The highest sum value of SOA_I
234 tracers over the SCS was 176 ng/m^3 , indicating strong photochemical formation of SOA from biogenic volatile
235 organics (Fig. 3). The geographical distribution of SOA_I tracers in this study was generally consistent with those
236 reported by Hu et al. (2013a), with higher concentrations of these tracers in atmospheric particles collected from
237 low-latitude oceanic zones (30° S – 30° N) due to large emissions from tropical forests and strong photochemical
238 reactions. Their reported average contents of SOA_I tracers in low-latitude oceanic zones fluctuated around
239 $9.2 \pm 6.7 \text{ ng/m}^3$, much lower than those measured in this study.

240 When the sum of SOA_I tracers in each sample was examined separately according to the air mass source, a
241 significant difference was found over the SCS between Category 1 ($85 \pm 66 \text{ ng/m}^3$) and Category 2 (19 ± 22
242 ng/m^3), with significance at $p < 0.01$. The average contribution of SOA_I tracers to TSP mass concentration over
243 the SYS was higher in category 1 ($0.4\% \pm 0.6\%$) than in category 2 ($0.06\% \pm 0.07\%$). The tracer values were
244 $2.7 \pm 1.8 \text{ ng/m}^3$ in Category 1 and $1.7 \pm 1.0 \text{ ng/m}^3$ in Category 2 over the NWPO, where no significant difference
245 between the two categories was found ($p > 0.05$). The average contribution of SOA_I tracers to TSP mass
246 concentration over the NWPO was higher in category 1 ($0.008\% \pm 0.005\%$) than that in category 2 ($0.005\% \pm$
247 0.005%). Supposed that concentrations of the tracers in Category 2 were completely contributed by marine
248 sources, it can be inferred that SOA_I carried by continental air masses increased sharply over the SCS. However,
249 it was not the case over the NWPO. Because all samples over the YBS fell into Category 1, this comparison
250 could not be made for the YBS.



251



252
253
254
255
256

Figure 3. Spatial distribution of SOA₁ tracer compounds over three marine regions, YBS and NWPO in 2014, SCS in 2017. The area of the pie indicates the concentration of total SOA₁ tracers. And the base map was from Resource and Environment Data Cloud Platform (<http://www.resdc.cn/DOI>), DOI: 10.12078/2018110201, © Institute of Geographic Sciences and Natural Resources Research, Chinese Academy of Sciences (CAS).~~The base map was from Resource and Environment Data Cloud Platform, DOI: 10.12078/2018110201.~~

257 3.3 Spatiotemporal distributions of SOA_M, SOA_s tracers

258 The sum of SOA_M tracers including HGA, HD-MGA, and MBTCA was greatest over the SCS region (3.5±6.0
259 ng/m³), where the concentration was approximately double that over the YBS (1.6±2.0 ng/m³) and NWPO
260 regions (1.6±2.7 ng/m³) (Fig. S1), but no significant differences were identified between any two campaigns.
261 The concentrations of SOA_M tracers were almost one magnitude lower than those of SOA_I tracers. Due to the
262 unique contribution of terpene-derived SOA to nucleation and growth of newly formed particles in the
263 atmosphere (Ehn et al., 2014; Gordon et al., 2017; Zhu et al., 2019), the SOA_M may primarily cause indirect
264 climate effects rather than direct effects of aerosols in the marine atmosphere. The difference in mean SOA_M
265 concentration between the SCS and NWPO narrowed to a factor of two, in contrast to the differences of
266 approximately one order of magnitude in mean SOA_I between the two types of atmospheres. The precursors of
267 SOA_M tracers derive mainly from coniferous forests (Duhl et al., 2008) and the decreasing proportion of
268 coniferous forests in subtropical and tropical regions may partially explain the smaller spatial difference in
269 SOA_M tracers over the SCS compared to the YBS and NWPO. However, the comparable SOA_M levels over the
270 YBS and NWPO have not yet been explained.

271 Only three SOA_M tracers were measured in this study, but other SOA_M tracers have been measured and reported
272 in marine atmospheres (Fu et al., 2011; Kang et al., 2018). In order to compare our results with the total amount
273 of SOA_M tracers in the literature, the total amounts measured in this study were multiplied by a factor of 3.1
274 (described in supporting information Sect. S1, Fig. S4) according to the chamber results obtained by Kleindienst
275 et al. (2007). The adjusted values over the SCS were closer to the mean of 11.6 ng/m³ observed over the East
276 China Sea (ECS) (Kang et al., 2018) and the lower values of 9.80–49.0 ng/m³ observed among 12 continental
277 sites in China (Ding et al., 2016). The adjusted total amounts of SOA_M over the NWPO and YBS were
278 comparable to previous observations of 3.0±5.0 ng/m³ collected from the Arctic to Antarctic in 2008-2010 (Hu
279 et al., 2013a), but much higher than observations of 63±49 pg/m³ over the North Pacific and Arctic in 2003
280 (Ding et al., 2013). This may also imply a substantial increase in SOA_M in the last decades, although more
281 investigations are needed to confirm this.

282 β-Caryophyllene is a major sesquiterpene emitted from plants such as Scots pine and European birch (Duhl et al.,
283 2008; Tarvainen et al., 2005). β-Caryophyllinic acid is formed through the ozonolysis or photo-oxidation of
284 β-caryophyllene. The highest levels of β-caryophyllinic acid were observed over the YBS (0.13±0.03 ng/m³),
285 followed by the SCS (0.08±0.11 ng/m³) and NWPO (0.05±0.09 ng/m³) (Fig. S1). The spatial distribution of
286 β-caryophyllinic acid clearly did not follow the general trend of biogenic SOA, with the highest values over the
287 SCS followed by the YBS. Compared to values from the literature, our results are much higher than those over
288 the North Pacific and Arctic Oceans (2.4±5.4 pg/m³) (Ding et al., 2013) but much lower than observations over
289 the East China Sea reported by Kang et al. (2018), where β-caryophyllinic acid was reported to be in the range
290 of 0.16–17.2 ng/m³ with a mean of 2.9 ng/m³. The large differences in β-caryophyllinic acid content observed in
291 various campaigns remain unexplained.

292 3.4 Spatiotemporal distributions of SOA_A tracers

293 When the concentrations of DHOPA in TSP were examined, the highest concentrations occurred over the SCS
294 (1.8±1.7 ng/m³), followed by the YBS (1.1±1.4 ng/m³), and the lowest values were recorded in the NWPO
295 region (0.3±0.5 ng/m³) (Fig. S1). The decreasing extent of the DHOPA from the SCS to the NWPO was
296 approximately three times less than that of SOA_I tracers but approximately three times larger than that of SOA_M

297 tracers. Ding et al. (2017) reported annual averages of DHOPA among various sites in China, which ranged from
298 1.2 to 8.8 ng/m³. The concentrations of DHOPA observed over the SCS and the YBS were similar to the lower
299 values observed in upwind continental atmospheres.

300 Formation of DHOPA depends on the molecular structures of aromatics, as well as concentrations of free
301 radicals and oxidants, etc. (Henze et al., 2008; Li et al., 2016). The mean value of DHOPA in Category 1
302 (0.43±0.65 ng/m³) was nearly twice that in Category 2 (0.20±0.31 ng/m³) over the NWPO ($p > 0.05$). With two
303 samples with high DHOPA (1.2, 2.1 ng/m³) in Category 1 to be excluded, the recalculated average DHOPA
304 decreases down to 0.17±0.21 ng/m³. The continent-derived DHOPA seemingly yielded a minor contribution to
305 the observed values over the NWPO, except during strong long-range transport episodes. Similarly, the mean
306 values of DHOPA were same in Category 1 (1.8±2.1 ng/m³) and Category 2 (1.8±1.5 ng/m³) samples collected
307 over the SCS and no significant difference was observed between two categories. Much stronger UV radiation
308 occurs over the SCS than the YBS, which may contribute to the elevated DHOPA level over the SCS. Aside
309 from continent-derived precursors, oil exploration and heavy marine traffic over the SCS are also potential
310 contributors to the higher DHOPA levels therein, and this link requires further investigation. Previous field
311 observations in China have demonstrated that biofuel or biomass combustion emissions act as important sources
312 of aromatics in the atmosphere (Zhang et al., 2016), as evidenced by the association between the nationwide
313 increase in DHOPA during the cold period and the enhancement of BB emissions (Ding et al., 2017). In this
314 study, no linear correlation was obtained between DHOPA and LEVO in samples collected over the SCS and the
315 other two campaigns, leaving emissions other than BB emissions, e.g., solvent use, oil exploration, marine
316 traffic, etc., as the major precursors for DHOPA in these marine atmospheres (Li et al., 2014).

317 3.5 Causes for high photochemical yields of SOA_I over the SCS

318 Because higher concentrations of SOA_I were observed in TSP samples collected over the SCS, the composition
319 of SOA_I tracers was further investigated in terms of their formation pathways and sources. Based on the results
320 of chamber experiments, Surratt et al. (2010) proposed different formation mechanisms for 2-MGA and MTLs.
321 2-MGA is a C₄-dihydroxycarboxylic acid, which forms through a high-NO_x pathway. MTLs and C₅-alkene
322 triols are mainly products of the photooxidation of epoxydiols of isoprene under low-NO_x conditions.

323 MTLs acted as the dominant compounds among SOA_I tracers in most TSP samples collected over the SCS, with
324 concentrations of 31±42 ng/m³ (Fig. 3). The ratio of 2-MGA/MTLs ranged from 0.2 to 3.1, with a median value
325 of 0.6. The ratio exceeded the unity in only 4 of 13 samples. This result allowed us to infer that the observed
326 SOA_I tracers were generated mainly under low-NO_x conditions. Although the concentration of
327 2-methylerythritol was nearly double that of 2-methylthreitol, they were highly correlated ($R^2 = 0.99$, $p < 0.05$)
328 because of their shared formation pathway. Satellite data showed that the NO₂ levels in South China and the
329 Philippines were low, except in a few hotspots (Fig. S2). Such low-NO_x conditions favor the formation of
330 MTLs rather than 2-MGA over the tropical SCS. The isoprene emitted from plants growing on oceanic islands
331 may also undergo chemical conversion to SOA under low-NO_x conditions, and low-NO_x conditions are always
332 expected in remote marine atmospheres (Davis et al., 2001).

333 In general, zonally and monthly averaged OH concentrations around 15°N are ~50% were greater than those
334 around 35 °N (Bahm and Khalil, 2004). Thus, enhanced formation of MTLs is theoretically expected under the
335 strong UV radiation of tropical regions. However, no significant correlation between the concentrations of
336 MTLs and UV radiation was obtained over the SCS (data not shown) possibly due to the influences of various
337 air masses. A field study showed that MTL yields were positively correlated with ambient temperature in
338 continental atmospheres (Ding et al., 2011). 2-MGA yields, in contrast, showed no significant correlation with

339 ambient temperature in this study. Moreover, lower relative humidity may enhance the formation of 2-MGA in
340 the particulate phase but not for MTLs (Zhang et al., 2011). Variation in ambient temperature and relative
341 humidity may complicate the relationship between the concentrations of SOA_I tracers and UV radiation over the
342 SCS.

343 In addition, the MTLs concentration in Category 1 (62 ± 55 ng/m³) was larger than that in Category 2 (11 ± 14
344 ng/m³). The more abundant MTLs associated with Category 1 was most likely related to long-range transport of
345 these chemicals from upwind continental areas, the oxidation of continental precursors in the marine atmosphere,
346 or both. Large emissions of isoprene were expected from tropical forests upwind of the SCS due to the high
347 vegetation coverage and high ambient temperature of such areas (Ding et al., 2011; Rinne et al., 2002). Global
348 estimates show tropical trees to be responsible for ~80% of terpenoid emissions and ~50% of other VOC
349 emissions (Guenther et al., 2012).

350 In a clean marine atmosphere, phytoplankton is the sole source of isoprene emissions over the oceans (Bonsang
351 et al., 1992; Broadgate et al., 1997). Chlorophyll-a has been widely employed as a measure of phytoplankton
352 abundance and a proxy for predicting isoprene concentrations in water (Hackenberg et al., 2017). The
353 satellite-derived chlorophyll-a level during the study period over the SCS was below 0.45 mg/m³, excluding
354 coastal areas (Fig. S3). The MTLs observation of 11 ± 14 ng/m³ in Category 2 should be considered as the upper
355 limitation value derived from marine phytoplankton in the SCS. Although air masses differed between
356 Categories 1 and 2, a good correlation was obtained between MTLs and 2-MGA when the data in the two
357 categories was pooled for analyses ($R^2 = 0.77$, $P < 0.01$). This strong correlation indicates these tracers are
358 primarily formed through shared pathways. However, this correlation was poor over the NWPO, as discussed
359 below.

360 3.6 Origin and formation of SOA_I over the NWPO

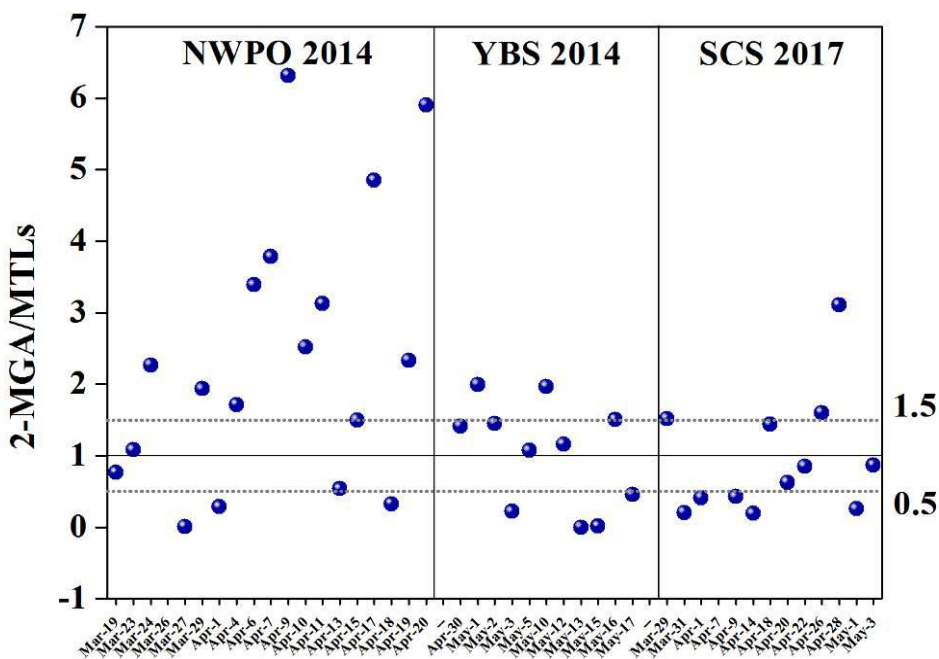
361 Over the NWPO, the concentration of 2-MGA was 1.6 ± 1.5 ng/m³, which was generally dominant among SOA_I
362 tracers, followed by MTLs (0.7 ± 0.3 ng/m³) and C5-alkene triols (0.03 ± 0.02 ng/m³). When the ratio of
363 2-MGA/MTLs was further examined, it varied greatly from <0.1 to 6.3, with a median value of 2.1. Most ratios
364 observed over the NWPO in this study were far greater than the values of 0.18–0.59 reported by Hu et al. (2013a)
365 from a global circumnavigation cruise, and also greater than 0.87–1.8 reported in urban areas of California
366 (Lewandowski et al., 2013) and the maximum value of 2.0 obtained over the YBS. Ding et al. (2013) also
367 reported ratios that fluctuated greatly from 0.5 to 10 with a median value of 3.3 during a summer cruise in the
368 NWPO and Arctic Ocean in 2003. The large 2-MGA/MTL ratios over the NWPO appeared to be highly
369 consistent over two independent sampling campaigns.

370 The compound profile of SOA_I tracers over the NWPO implied high-NO_x conditions allowing oxidation of
371 isoprene to generate the SOA_I present in most samples. Such high-NO_x conditions are impossible in a remote
372 marine atmosphere, as indicted in Figure S2. Given that the lifespan of isoprene in the atmosphere is only
373 several hours (Bonsang et al., 1992), the long-range transport of oxidation products formed under high NO_x
374 levels over the continents likely led to the 2-MGA-dominated composition of SOA_I. Based on air mass back
375 trajectories, this long-range transport may involve 2-MGA originating from Siberia, northeastern China, or
376 Japan.

377 Organic aerosols over the NWPO were strongly influenced by forest fires that take place in Siberia during
378 spring and summer almost every year (Ding et al., 2013; Huang et al., 2009). Previous emissions inventory
379 studies have reported high isoprene and NO_x emissions from various BB types (Akagi et al., 2011; Andreae and
380 Merlet, 2001). Ding et al. (2013) thus argued that an increase in emissions of isoprene in the presence of BB,

381 followed by its chemical conversion under high-NO_x conditions, may lead to transport over thousands of
 382 kilometers and hold at the detectable concentrations in the remote marine atmosphere over the NWPO. The
 383 same argument may hold true for the elevated ratios of 2-MGA/MTLs observed over the NWPO in this study
 384 (Fig. 4). However, we did not find a significant correlation between 2-MGA and LEVO over the NWPO. The
 385 decomposition of LEVO reported in literature (Fraser and Lakshmanan, 2000; Hennigan et al., 2010; Hoffmann
 386 et al., 2010) may lower the correlation between them. However, whether 2-MGA can decompose in ambient air
 387 remains poorly understood.

388 On the other hand, the ratios of 2-MGA/MTLs in 3 of 19 samples collected over the NWPO were below 0.5
 389 (Figure 4). In these cases, the oxidation of isoprene under low-NO_x conditions likely dominated the generation
 390 of SOA_I. The ratios of 2-MGA/MTLs were 0.5–1.5 in 4 of 19 samples, suggesting mixed contributions to SOA_I
 391 from the oxidation of isoprene under low-NO_x conditions and high-NO_x conditions. As the major formation
 392 pathways of 2-MGA and MTLs varied greatly among samples, no significant correlation ($R^2 = 0.12$, $p > 0.05$)
 393 was obtained between 2-MGA and MTLs over the NWPO. Recall that the tracer values of SOA_I were 2.7 ± 1.8
 394 ng/m³ in Category 1 and 1.7 ± 1.0 ng/m³ in Category 2. This implied that SOA_I derived from marine sources was
 395 comparable to that derived from the continent outflows.



396
 397 **Figure 4. Spatial ratio of 2-MGA/MTLs among SOA_I tracers over three marine regions.**

398 3.7 Source apportionment of secondary organic carbon (SOC)

399 The tracer-based approach developed by Kleindienst et al. (2007) was applied to estimate the concentrations of
 400 SOC and WSOC_{BB}, as follows:

$$401 \quad [SOC] = \frac{\sum_i [tri]}{f_{SOC}} \quad (1)$$

$$402 \quad [WSOC_{BB}] = \frac{C_{tracer}}{f_{tracer/WSOC_{BB}}} \quad (2)$$

403 where $\Sigma_i(\text{tri})$ is the sum of concentrations of the selected suite of tracers for a precursor, and f_{SOC} is the mass
404 fraction of tracer compounds in SOC generated from the precursor in chamber experiments. Assuming that the
405 f_{SOC} values in ambient air match those in the chamber, the f_{SOC} values for precursors such as isoprene,
406 monoterpenes, β -caryophyllene, and aromatics were $0.155 \pm 0.039 \mu\text{g}/\mu\text{gC}$, $0.231 \pm 0.111 \mu\text{g}/\mu\text{gC}$, 0.023 ± 0.0046
407 $\mu\text{g}/\mu\text{gC}$, and $0.00797 \pm 0.0026 \mu\text{g}/\mu\text{gC}$, respectively (Kleindienst et al., 2007), with uncertainty described in
408 Sect. S2. The fraction of LEVO in WSOC ($0.0994 \mu\text{g}/\mu\text{gC}$) from the BB plume was used for WSOC_{BB} (Ding et
409 al., 2008). The f_{SOC} value for monoterpenes was scaled up by a factor of 3.1 based on experimental observations,
410 as these two tracers (HGA+HD-MGA) accounted for 2/9 of the total tracers of monoterpenes, as described in
411 the supporting information (Kleindienst et al., 2007).

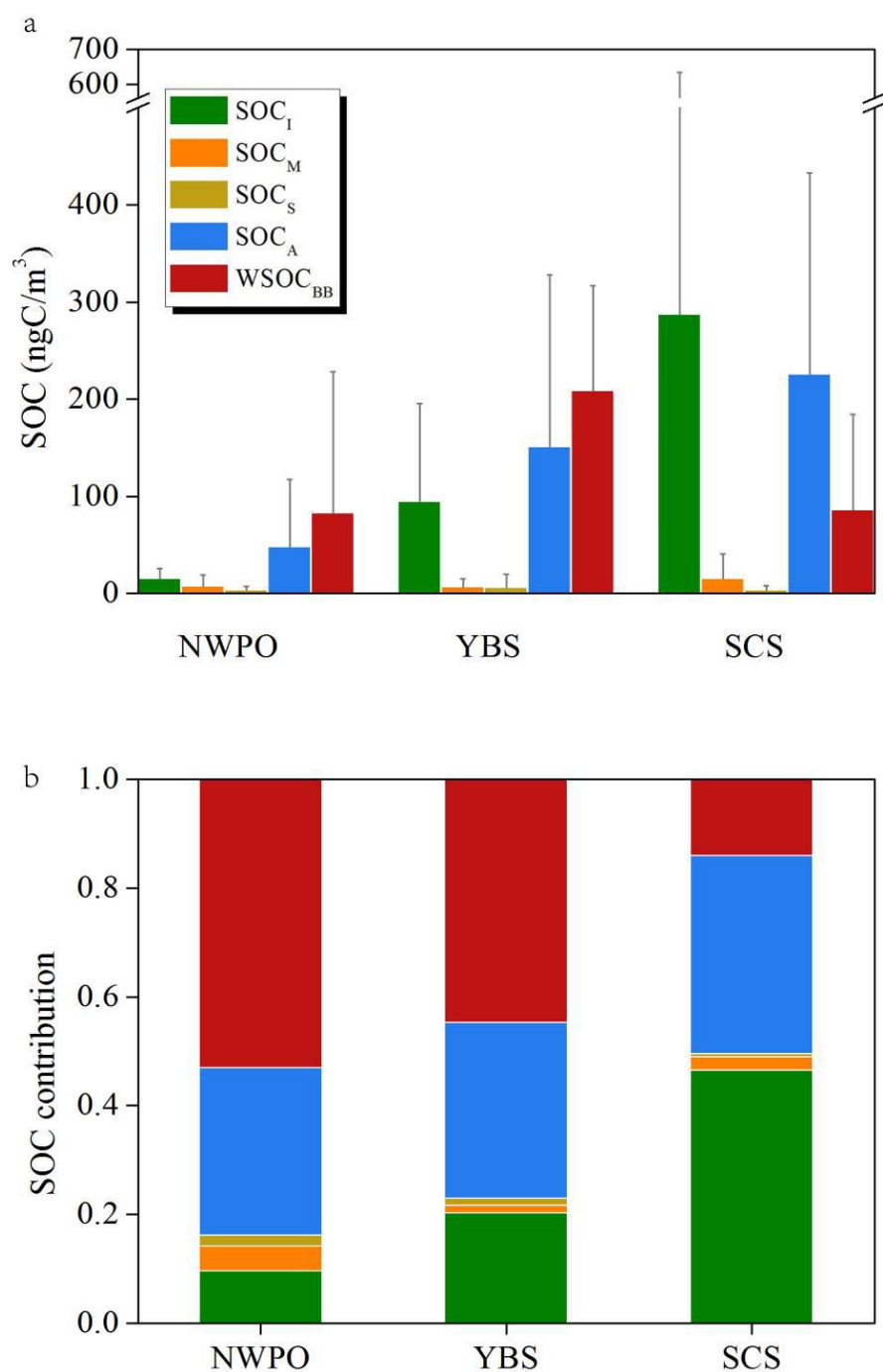
412 Over the SCS, nearly half of the sum of SOC and WSOC_{BB} was in the form of SOC_I (47%), followed by SOC_A
413 (36%), WSOC_{BB} (14%) and a minor contribution of 2.5% from SOC_M (Fig. 5). This composition pattern over
414 the SCS could be attributed to abundant biogenic SOA formation in low-latitude tropical marine atmospheres.
415 Over tropical marine regions, atmospheric oxidation products can account for 47–59% of the total organic
416 content estimated, with biomass burning emissions making up only 2–7% based on source apportionment using
417 organic tracers (Fu et al., 2011). A model study by Fu et al. (2012) showed that secondary formation accounts
418 for as much as 62% of OC estimated using tracers in eastern China in summer. A reverse pattern was observed
419 over the YBS, with WSOC_{BB} as the dominant contributor (45%) to the sum of SOC and WSOC_{BB}, followed by
420 SOC_A (32%) and SOC_I (20%). The contribution of SOC_M was also minor, at 1.5%. Notably, the chemical
421 composition observed over the NWPO was similar to that over the YBS, with WSOC_{BB} contributing up to 53%.
422 In addition, Kang et al. (2018) used the PMF method to identify various sources of OC in marine aerosols over
423 the ECS such as secondary nitrate, BSOA, BB, and fungal spores.

424 Geographically, the estimated SOC values from BVOCs ranked at the highest level of $306 \pm 343 \text{ ngC}/\text{m}^3$ over the
425 SCS, decreasing to $107 \pm 99 \text{ ngC}/\text{m}^3$ over the YBS and $24 \pm 22 \text{ ngC}/\text{m}^3$ over the NWPO. The estimates of
426 aromatic SOC exhibited the same geographic trend, with values of $225 \pm 208 \text{ ngC}/\text{m}^3$ over the SCS, 151 ± 177
427 ngC/m^3 over the YBS and $48 \pm 69 \text{ ngC}/\text{m}^3$ over the NWPO. Recent modeling results have also shown that
428 aromatic emissions are the predominant precursors of SOA during springtime in China in comparison with
429 BVOCs and other AVOCs (Han et al., 2016). Among estimates of WSOC_{BB}, the highest values of 209 ± 108
430 ngC/m^3 were recorded over the YBS, followed by comparable levels of $86 \pm 98 \text{ ngC}/\text{m}^3$ (SCS) and 83 ± 145
431 ngC/m^3 (NWPO).

432 In our study, the calculated WSOC_{BB} estimate accounted for $4.1 \pm 5.0\%$ and $3.3 \pm 1.7\%$ of measured OC over the
433 NWPO and YBS, respectively, and these values are higher than that obtained over the ECS during summer
434 (1.4%) (Kang et al., 2018). Estimated SOC from BVOCs accounted for only $1.5 \pm 1.4\%$ and $1.8 \pm 1.7\%$ to the
435 measured OC over the NWPO and YBS, respectively, which is lower than that over ECS (4.21%) (Kang et al.,
436 2018). However, the mean values obtained in this study were similar to the total SOC level estimated using
437 tracers as a proportion of measured WSOC (4%) during a cruise on the North Pacific and Arctic Oceans,
438 supposed that WSOC accounted for half of the total OC in atmospheric particles (Ding et al., 2013).

439 The calculated SOC level derived from organic tracers accounted for less than 8% of total measured OC in these
440 study areas. However, these SOC compounds are expected to derive mainly from photochemical reactions in the
441 gas phase, followed by gas-aerosol partitioning. These compounds likely play an important role in the growth of
442 newly formed particles alongside pre-existing nucleation mode or Aitken mode particles. However, most organic
443 matter detected in bulk samples may originate from primary sources, heterogeneous reactions and in-cloud
444 processing (Ervens et al., 2011; Kanakidou et al., 2005; Nichols, 2016), and these compounds may be major
445 drivers of the direct climate effects of aerosols, rather than indirect climate effects. In the future, a
446 comprehensive combination measurement of organic tracers and organic matter with an aerosol mass

447 spectrometer should be used to elucidate the formation and growth processes of atmospheric nanoparticles.
448



449
450 **Figure 5. Average SOC levels calculated using the tracer-SOC/WSOC method over three marine regions**
451 **(YBS and NWPO in 2014, SCS in 2017) and their contributions based on five organic tracers measured in**
452 **this study.**

453 4. Conclusions

454 This study investigated the geographical distributions of tracer-based organic matter observations in TSP
455 collected over two marginal seas of China and the NWPO in the spring season, when the East Asian monsoon
456 carries biogenic and anthropogenic aerosols over these oceanic zones. We found a significantly large difference

457 in LEVO over the NWPO between two categories of air masses originating from upwind continents or oceanic
458 regions, as Category 1 (continental) contained $13 \pm 18 \text{ ng/m}^3$ and Category 2 (oceanic) had $2.0 \pm 1.8 \text{ ng/m}^3$; the
459 concentrations of LEVO in Category 2 were closer to the low values reported in the literature. This further
460 implied a large increase in continent-derived BB aerosols in marine atmospheres over the NWPO in recent
461 decades, compared to previous studies. An important question is thereby raised, i.e., does a large increase in
462 continent-derived BB aerosols in marine atmospheres over the NWPO occur continuously and largely in recent
463 decades? Combining the L/M ratios of 19 ± 4 over the NWPO with the calculated air mass back trajectories
464 indicates that the increase was very likely associated with enhanced emissions of BB aerosols from wildfires in
465 Siberia and northeastern China. Moreover, the mean level of BB aerosols over the SCS nearly matched that over
466 the NWPO. The contents of LEVO in Category 2 air masses, derived from oceanic zones over the SCS, were
467 comparable with those reported in the literature, but the mean value was only about a quarter of that in Category
468 1, representing air masses from upwind continents. However, the limited data available over the SCS in the
469 literature cannot support inferences about whether BB aerosols emitted from upwind tropical forests have
470 increased in recent decades.

471 The concentrations of SOA_I over the SCS were approximately one order of magnitude greater than those
472 observed over the NWPO and several times larger than those over the YBS. The larger values observed over the
473 SCS in Category 1 than in Category 2 were likely driven by high emissions of isoprene from upwind tropical
474 forests and strong solar radiation. The MTLs dominance of SOA_I over the SCS strongly suggested that SOC
475 from BVOCs was generated primarily under low- NO_x conditions. On the other hand, 2-MGA dominance over
476 the YBS implied that most SOC was generated under high- NO_x conditions. Elevated ratios of 2-MGA/MTLs
477 of >1.5 were obtained for 11 of 19 total samples collected over the NWPO, consistent with those reported in the
478 literature. Larger ratios may be attributed to possible emissions of BVOCs in the presence of BB. However, the
479 comparable concentrations of SOA_I in Category 1 and Category 2 samples collected over the NWPO implied a
480 large contribution of SOA_I from marine sources. The aromatic SOA tracers' levels were highest over the SCS,
481 followed by values obtained over the YBS and NWPO. The high values observed over the SCS may be related
482 to strong solar radiation, but the sources of precursors remain unexplained. Based on the concentrations in
483 Category 1 and 2 air samples collected over the SCS and NWPO, mixed sources of aromatic VOCs should exist,
484 including continent-derived precursors, oil exploration and heavy marine traffic.

485 Over the NWPO and the YBS, the estimated WSOC_{BB} levels were nearly equal to the sum of SOC estimated
486 from the oxidation of aromatics and BVOCs. Over the SCS, SOC estimated from the oxidation of BVOCs was
487 significantly larger than the estimated WSOC_{BB} . The geographical difference may be related to emissions of
488 primary particulate organics and gaseous precursors as well as formation processing of secondary organics in
489 various atmospheres.

490 The atmospheric composition of SOA in different geographical locations is, however, highly complex and is
491 regulated by many factors including local meteorological conditions, anthropogenic emissions, plant species,
492 vegetation cover and regional chemistry, and therefore warrants further quantification and analyses. Particularly,
493 whether BB aerosols and other biogenic organic aerosols in marine atmospheres will continuously increase
494 under warming conditions.

495 **Table 1. Sum of organic tracer contents (ng/m³) at different locations worldwide.**

Site	Date	Sampler	LEVO	SOA _I	SOA _M	SOA _S	SOA _A	Reference
Wakayama, Japan (Forest)	August 20–30, 2010, Day	TSP	2.5±2.1	281±274	54.6±50.2	1.2±1.2		(Zhu et al., 2016a)
	Night		1.1±0.9	199±207	36.3±33.6	0.9±0.8		
Across China	summer 2012	Anderson sampler		123±79	10.5±6.6	5.0±4.0	2.9±1.5	(Ding et al., 2014)
Beijing (PKU) (urban site)	summer 2007	PM2.5	37-148	59±32	30±14	2.7±1.0		(Yang et al., 2016)
Beijing (YUFA) (suburban site)			34-149	75±43	32±14	3.9±1.5		
Shanghai (BS) (Suburban site)	Apr-May 2010	PM2.5	88.8±57.2	3.8±3.9	6.1±3.7	1.0±0.7	1.1±0.7	(Feng et al., 2013)
Shanghai (XJH) (Urban site)			58.3±27.5	2.5±1.7	2.7±1.3	0.4±0.3	0.6±0.4	
Mt. Tai	summer 2014	PM2.5		56.4±45.6	34.4±28.4			(Zhu et al., 2017)
Central Pearl River Delta	fall-winter 2007	PM2.5		30.8±15.9	6.6±4.4	0.5±0.6		(Ding et al., 2011)
Central Tibetan Plateau	2012-2013	Anderson sampler		26.6±44.2	1.0±0.6	0.09±0.1	0.3±0.2	(Shen et al., 2015)
Mumbai, India	winter 2007	PM10		4.1±2.4	29±22		0.6±0.6	(Fu et al., 2016)
	summer 2007			1.1±0.7	9.4±4.7		0.05±0.1	
Alaska	Spring 2009	TSP		2.4	3.6	0.9		(Haque et al., 2016)
	2008-2009	TSP		4.1	2.0	1.5		
SYS	Spring 2017	TSP	9.6±8.6	45±54	3.5±6.0	0.07±0.1	1.8±1.7	This study
YBS	Spring 2014	TSP	21±11	15±16	1.6±2.0	0.1±0.3	1.1±1.4	This study
NWPO	Spring 2014	TSP	8.2±14	2.3±1.6	1.6±2.7	0.05±0.09	0.3±0.5	This study
East China Sea	18 May to 12 June 2014	TSP	0.09–64.3 (7.3)	0.15–64.0 (8.4)	0.26–87.2 (11.6)	0.16–17.2 (2.9)		(Kang et al., 2018)
Arctic to Antarctic	July to September 2008; November 2009 to April 2010	TSP	5.4±6.2	8.5±11	3.0±5.0			(Hu et al., 2013a; Hu et al., 2013b)
North Pacific	2003	TSP		0.5±0.4	0.6±0.4	0.06±0.05	0.002±0.005	(Ding et al., 2013)

497 **Data availability.** Most of the data are shown in supplement. Other data are available by contacting the
498 corresponding author.

499 **Supplement.** The supplement related to this article is available.

500 **Author contributions.** XY, TG and JF conceived and led the studies. TG, JW and JF carried out the
501 experiments and analyzed the data. TG and JF interpreted the results. ZG, JF, HG discussed the results and
502 commented on the manuscript. TG prepared the manuscript with contributions from all the co-authors.

503 **Competing interests.** The authors declare that they have no conflict of interest.

504 **Acknowledgements.** This research has been supported by the National Key Research and Development
505 Program in China (No.2016YFC0200504) and the Natural Science Foundation of China (Grant No. 41576118,
506 41473088).

507

508 **References:**

- 509 Ait-Helal, W., Borbon, A., Sauvage, S., de Gouw, J. A., Colomb, A., Gros, V., Freutel, F., Crippa, M., Afif, C.,
510 Baltensperger, U., Beekmann, M., Doussin, J.-F., Durand-Jolibois, R., Fronval, I., Grand, N., Leonardis, T.,
511 Lopez, M., Michoud, V., Miet, K., Perrier, S., Prévôt, A. S. H., Schneider, J., Siour, G., Zapf, P., and Locoge, N.:
512 Volatile and intermediate volatility organic compounds in suburban Paris: variability, origin and importance for
513 SOA formation, *Atmos. Chem. Phys.*, 14, 10439-10464, <https://doi.org/10.5194/acp-14-10439-2014>, 2014.
- 514 Akagi, S. K., Yokelson, R. J., Wiedinmyer, C., Alvarado, M. J., Reid, J. S., Karl, T., Crouse, J. D., and
515 Wennberg, P. O.: Emission factors for open and domestic biomass burning for use in atmospheric models,
516 *Atmos. Chem. Phys.*, 11, 4039-4072, <https://doi.org/10.5194/acp-11-4039-2011>, 2011.
- 517 Andreae, M. O. and Merlet, P.: Emission of trace gases and aerosols from biomass burning, *Global Biogeochem.*
518 *Cy.*, 15, 955-966, 2001.
- 519 Arnold, S. R., Spracklen, D. V., Williams, J., Yassaa, N., Sciare, J., Bonsang, B., Gros, V., Peeken, I., Lewis, A.
520 C., Alvain, S., and Moulin C.: Evaluation of the global oceanic isoprene source and its impacts on marine
521 organic carbon aerosol, *Atmos. Chem. Phys.*, 9, 1253-1262, 2009.
- 522 Bahm, K. and Khalil, M. A. K.: A new model of tropospheric hydroxyl radical concentrations, *Chemosphere*, 54,
523 143-166, <https://doi.org/143-166>, 10.1016/j.chemosphere.2003.08.006, 2004.
- 524 Bao, H., Niggemann, J., Luo, L., Dittmar, T., and Kao, S.: Molecular composition and origin of water-soluble
525 organic matter in marine aerosols in the Pacific off China, *Atmos. Environ.*, 191, 27-35,
526 <https://doi.org/10.1016/j.atmosenv.2018.07.059>, 2018.
- 527 Bonsang, B., Polle, C., and Lambert, G.: Evidence for marine production of isoprene, *Geophys. Res. Lett.*, 19,
528 1129-1132, 1992.
- 529 Bougiatioti, A., Bezantakos, S., Stavroulas, I., Kalivitis, N., Kokkalis, P., Biskos, G., Mihalopoulos, N.,
530 Papayannis, A., and Nenes, A.: Biomass-burning impact on CCN number, hygroscopicity and cloud formation
531 during summertime in the eastern Mediterranean, *Atmos. Chem. Phys.*, 16, 7389-7409,
532 <https://doi.org/10.5194/acp-16-7389-2016>, 2016.
- 533 Broadgate, W. J., Liss, P. S., and Penkett, S. A.: Seasonal emissions of isoprene and other reactive hydrocarbon
534 gases from the ocean, *Geophys. Res. Lett.*, 24, 2675-2678, 1997.

535 Chen, J., Li, C., Ristovski, Z., Milic, A., Gu, Y., Islam, M. S., Wang, S., Hao, J., Zhang, H., He, C., Guo, H., Fu,
536 H., Miljevic, B., Morawska, L., Thai, P., LAM, Y. F., Pereira, G., Ding, A., Huang, X., and Dumka, U. C.: A
537 review of biomass burning: Emissions and impacts on air quality, health and climate in China, *Sci. Total*
538 *Environ.*, 579, 1000-1034, <https://doi.org/10.1016/j.scitotenv.2016.11.025>, 2017.

539 Claeys, M., Graham, B., Vas, G., Wang, W., Vermeylen, R., Pashynska, V., Cafmeyer, J., Guyon, P., Andreae,
540 M. O., Artaxo, P., and Maenhaut, W.: Formation of secondary organic aerosols through photooxidation of
541 isoprene, *Science*, 303, 1173-1176, 2004.

542 Claeys, M., Wang, W., Vermeylen, R., Kourtchev, I., Chi, X., Farhat, Y., Surratt, J. D., Gómez-González, Y.,
543 Sciare, J., and Maenhaut, W.: Chemical characterisation of marine aerosol at Amsterdam Island during the
544 austral summer of 2006–2007, *J. Aerosol Sci.*, 41, 13-22, <https://doi.org/10.1016/j.jaerosci.2009.08.003>, 2010.

545 Davis, D. D., Grodzinsky, G., Kasibhatla, P., Crawford, J., Chen, G., Liu, S., Bandy, A., Thornton, D., Guan, H.,
546 and Sandholm, S.: Impact of ship emissions on marine boundary layer NO_x and SO₂ distributions over the
547 Pacific Basin, *Geophys. Res. Lett.*, 28, 235-238, 2001.

548 Ding, X., Zheng, M., Yu, L., Zhang, X., Weber, R. J., Yan, B., Russell, A. G., Edgerton, E. S., and Wang, X.:
549 Spatial and seasonal trends in biogenic secondary organic aerosol tracers and water-soluble organic carbon in
550 the southeastern United States, *Environ. Sci. Technol.*, 42, 5171-5176, <https://doi.org/10.1021/es7032636>, 2008.

551 Ding, X., Wang, X., and Zheng, M.: The influence of temperature and aerosol acidity on biogenic secondary
552 organic aerosol tracers: Observations at a rural site in the central Pearl River Delta region, South China, *Atmos.*
553 *Environ.*, 45, 1303-1311, <https://doi.org/10.1016/j.atmosenv.2010.11.057>, 2011.

554 Ding, X., Wang, X., Xie, Z., Zhang, Z., and Sun, L.: Impacts of Siberian biomass burning on organic aerosols
555 over the North Pacific Ocean and the Arctic: Primary and secondary organic tracers, *Environ. Sci. Technol.*, 47,
556 3149-3157, <https://doi.org/10.1021/es3037093>, 2013.

557 Ding, X., He, Q., Shen, R., Yu, Q., and Wang, X.: Spatial distributions of secondary organic aerosols from
558 isoprene, monoterpenes, β -caryophyllene, and aromatics over China during summer, *J. Geophys. Res.-Atmos.*,
559 119, 877-891, <https://doi.org/10.1002/2014JD021748>, 2014.

560 Ding, X., Zhang, Y., He, Q., Yu, Q., Shen, R., Zhang, Y., Zhang, Z., Lyu, S., Hu, Q., Wang, Y., Li, L., Song,
561 W., and Wang, X.: Spatial and seasonal variations of secondary organic aerosol from terpenoids over China, *J.*
562 *Geophys. Res.-Atmos.*, 121, 661-678, <https://doi.org/10.1002/2016JD025467>, 2016.

563 Ding, X., Zhang, Y., He, Q., Yu, Q., Wang, J., Shen, R., Song, W., Wang, Y., and Wang, X.: Significant
564 increase of aromatics-derived secondary organic aerosol during fall to winter in China, *Environ. Sci. Technol.*,
565 51, 7432-7441, <https://doi.org/10.1021/acs.est.6b06408>, 2017.

566 Duhl, T. R., Helmig, D., and Guenther, A.: Sesquiterpene emissions from vegetation: a review, *Biogeosciences*,
567 5, 761–777, <https://doi:10.5194/bg-5-761-2008>, 2008,

568 Ehn, M., Thornton, J. A., Kleist, E., Sipilä, M., Junninen, H., Pullinen, I., Springer, M., Rubach, F., Tillmann, R.,
569 Lee, B., Lopez-Hilfiker, F., Andres, S., Acir, I.-H., Rissanen, M., Jokinen, T., Schobesberger, S., Kangasluoma,
570 J., Kontkanen, J., Nieminen, T., Kurtén, T., Nielsen, L. B., Jørgensen, S., Kjaergaard, H. G., Canagaratna, M.,
571 Dal Maso, M., Berndt, T., Petäjä, T., Wahner, A., Kerminen, V.-M., Kulmala, M., Worsnop, D. R., Wildt, J.,
572 and Mentel, T. F.: A large source of low volatility secondary organic aerosol, *Nature*, 506, 476–479,
573 <https://doi.org/10.1038/nature13032>, 2014.

574 Ekström, S., Nozière, B., and Hansson, H.: The Cloud Condensation Nuclei (CCN) properties of 2-methyltetrols
575 and C3-C6 polyols from osmolality and surface tension measurements, *Atmos. Chem. Phys.*, 9, 973-980, 2009.

576 Ervens, B., Turpin, B. J., and Weber, R. J.: Secondary organic aerosol formation in cloud droplets and aqueous
577 particles (aqSOA): a review of laboratory, field and model studies, *Atmos. Chem. Phys.*, 11, 11069-11102,
578 <https://doi.org/10.5194/acp-11-11069-2011>, 2011.

579 Feng, J. L., Guo, Z. G., Zhang, T. R., Yao, X. H., Chan, C. K., and Fang, M.: Source and formation of
580 secondary particulate matter in PM_{2.5} in Asian continental outflow, *J. Geophys. Res.-Atmos.*, 117, D03302,
581 <https://doi.org/10.1029/2011JD016400>, 2012.

582 Feng, J., Li, M., Zhang, P., Gong, S., Zhong, M., Wu, M., Zheng, M., Chen, C., Wang, H., and Lou, S.:

583 Investigation of the sources and seasonal variations of secondary organic aerosols in PM_{2.5} in Shanghai with
584 organic tracers, *Atmos. Environ.*, 79, 614-622, <https://doi.org/10.1016/j.atmosenv.2013.07.022>, 2013.

585 Fraser, M. P. and Lakshmanan, K.: Using levoglucosan as a molecular marker for the long-range transport of
586 biomass combustion aerosols, *Environ. Sci. Technol.*, 34, 4560-4564, <https://doi.org/10.1021/es9912291>, 2000.

587 Fu, P., Kawamura, K., and Miura, K.: Molecular characterization of marine organic aerosols collected during a
588 round-the-world cruise, *J. Geophys. Res.-Atmos.*, 116, D13302, <https://doi.org/10.1029/2011JD015604>, 2011.

589 Fu, P., Aggarwal, S. G., Chen, J., Li, J., Sun, Y., Wang, Z., Chen, H., Liao, H., Ding, A., Umarji, G. S., Patil, R.
590 S., Chen, Q., and Kawamura, K.: Molecular markers of secondary organic aerosol in Mumbai, India, *Environ.*
591 *Sci. Technol.*, 50, 4659-4667, <https://doi.org/10.1021/acs.est.6b00372>, 2016.

592 Fu, T. M., Cao, J. J., Zhang, X. Y., Lee, S. C., Zhang, Q., Han, Y. M., Qu, W. J., Han, Z., Zhang, R., Wang, Y.
593 X., Chen, D., and Henze, D. K.: Carbonaceous aerosols in China: top-down constraints on primary sources and
594 estimation of secondary contribution, *Atmos. Chem. Phys.*, 12, 2725-2746,
595 <https://doi.org/10.5194/acp-12-2725-2012>, 2012.

596 Gantt, B., Meskhidze, N., and Kamykowski, D.: A new physically-based quantification of marine isoprene and
597 primary organic aerosol emissions, *Atmos. Chem. Phys.*, 9, 4915-4927,
598 <https://doi.org/10.5194/acp-9-4915-2009>, 2009.

599 Generoso, S., Bey, I., Attié, J., and Bréon, F.: A satellite- and model-based assessment of the 2003 Russian fires:
600 Impact on the Arctic region, *J. Geophys. Res.-Atmos.*, 112, D15302, <https://doi.org/10.1029/2006JD008344>,
601 2007.

602 Gordon, H., Kirkby, J., Baltensperger, U., Bianchi, F., Breitenlechner, M., Curtius, J., Dias, A., Dommen, J.,
603 Donahue, N. M., Dunne, E. M., Duplissy, J., Ehrhart, S., Flagan, R. C., Frege, C., Fuchs, C., Hansel, A., Hoyle,
604 C. R., Kulmala, M., Kürten, A., Lehtipalo, K., Makhmutov, V., Molteni, U., Rissanen, M. P., Stozkhov, Y.,
605 Tröstl, J., Tsagkogeorgas, G., Wagner, R., Williamson, C., Wimmer, D., Winkler, P. M., Yan, C., and Carslaw,
606 K. S.: Causes and importance of new particle formation in the present-day and preindustrial atmospheres, *J.*
607 *Geophys. Res.-Atmos.*, 122, 8739-8760, <https://doi.org/10.1002/2017JD026844>, 2017.

608 Guenther, A., Hewitt, C. N., Erickson, D., Fall, R., Geron, C., Graedel, T., Harley, P., Klinger, L., Lerdau, M.,
609 McKay, W. A., Pierce T., Scholes B., Steinbrecher R., Tallamraju R., Taylor J., and Zimmerman P.: A global
610 model of natural volatile organic compound emissions, *J. Geophys. Res.-Atmos.*, 100, 8873-8892, 1995.

611 Guenther, A., Karl, T., Harley, P., Wiedinmyer, C., Palmer, P. I., and Geron, C.: Estimates of global terrestrial
612 isoprene emissions using MEGAN (Model of Emissions of Gases and Aerosols from Nature), *Atmos. Chem.*
613 *Phys.*, 6, 3181-3210, 2006.

614 Guenther, A. B., Jiang, X., Heald, C. L., Sakulyanontvittaya, T., Duhl, T., Emmons, L. K., and Wang, X.: The
615 Model of Emissions of Gases and Aerosols from Nature version 2.1 (MEGAN2.1): an extended and updated
616 framework for modeling biogenic emissions, *Geosci. Model Dev.*, 5, 1471-1492,
617 <https://doi.org/10.5194/gmd-5-1471-2012>, 2012.

618 Hackenberg, S. C., Andrews, S. J., Airs, R., Arnold, S. R., Bouman, H. A., Brewin, R. J. W., Chance, R. J.,
619 Cummings, D., Dall'Olmo, G., Lewis, A. C., Minaeian, J. K., Reifel, K. M., Small, A., Tarran, G. A., Tilstone,
620 G. H., and Carpenter, L. J.: Potential controls of isoprene in the surface ocean, *Global Biogeochem. Cy.*, 31,
621 644-662, <https://doi.org/10.1002/2016GB005531>, 2017.

622 Han, Z., Xie, Z., Wang, G., Zhang, R., and Tao, J.: Modeling organic aerosols over east China using a volatility
623 basis-set approach with aging mechanism in a regional air quality model, *Atmos. Environ.*, 124, 186-198,
624 <https://doi.org/10.1016/j.atmosenv.2015.05.045>, 2016.

625 Haque, M. M., Kawamura, K., and Kim, Y.: Seasonal variations of biogenic secondary organic aerosol tracers in
626 ambient aerosols from Alaska, *Atmos. Environ.*, 130, 95-104, 2016.

627 Heald, C. L., Henze, D. K., Horowitz, L. W., Feddema, J., Lamarque, J.-F., Guenther, A., Hess, P. G., Vitt, F.,
628 Seinfeld, J. H., Goldstein, A. H., and Fung, I.: Predicted change in global secondary organic aerosol
629 concentrations in response to future climate, emissions, and land use change, *J. Geophys. Res.-Atmos.*, 113,
630 D05211, <https://doi.org/10.1029/2007JD009092>, 2008.

631 Hennigan, C. J., Sullivan, A. P., Collett Jr., J. L. and Robinson, A. L.: Levoglucosan stability in biomass
632 burning particles exposed to hydroxyl radicals, *Geophys. Res. Lett.*, 37, L09806,
633 <https://doi.org/10.1029/2010GL043088>, 2010.

634 Henze, D. K., Seinfeld, J. H., Ng, N. L., Kroll, J. H., Fu, T.-M., Jacob, D. J., and Heald, C. L.: Global modeling
635 of secondary organic aerosol formation from aromatic hydrocarbons: high-vs. low-yield pathways, *Atmos.*
636 *Chem. Phys.*, 8, 2405-2420, 2008.

637 Hoffmann, D., Tilgner, A., Iinuma, Y. and Herrmann, H.: Atmospheric stability of levoglucosan: A detailed
638 laboratory and modeling study, *Environ. Sci. Technol.*, 44, 694-699, <https://doi.org/10.1021/es902476f>, 2010.

639 Hsiao, T., Ye, W., Wang, S., Tsay, S., Chen, W., Lin, N., Lee, C., Hung, H., Chuang, M., and Chantara, S.:
640 Investigation of the CCN activity, BC and UVBC mass concentrations of biomass burning aerosols during the
641 2013 BASELInE campaign, *Aerosol Air Qual. Res.*, 16, 2742-2756, <https://doi.org/10.4209/aaqr.2015.07.0447>,
642 2016.

643 Hu, D. and Yu, J. Z.: Secondary organic aerosol tracers and malic acid in Hong Kong: seasonal trends and
644 origins, *Environ. Chem.*, 10, 381-394, <https://doi.org/10.1071/EN13104>, 2013.

645 Hu, Q., Xie, Z., Wang, X., Kang, H., He, Q., and Zhang, P.: Secondary organic aerosols over oceans via
646 oxidation of isoprene and monoterpenes from Arctic to Antarctic, *Sci. Rep.-UK*, 3, 2280,
647 <https://doi.org/10.1038/srep02280>, 2013a.

648 Hu, Q., Xie, Z., Wang, X., Kang, H., and Zhang, P.: Levoglucosan indicates high levels of biomass burning
649 aerosols over oceans from the Arctic to Antarctic, *Sci. Rep.-UK*, 3, 3119, <https://doi.org/10.1038/srep03119>,
650 2013b.

651 Hu, Q., Qu, K., Gao, H., Cui, Z., Gao, Y., and Yao, X.: Large increases in primary trimethylaminium and
652 secondary dimethylaminium in atmospheric particles associated with cyclonic eddies in the Northwest Pacific
653 Ocean, *J. Geophys. Res.-Atmos.*, 123, 133-146, <https://doi.org/10.1029/2018JD028836>, 2018.

654 Huang, S., Siebert, F., Goldammer, J. G., and Sukhinin, A. I.: Satellite-derived 2003 wildfires in southern
655 Siberia and their potential influence on carbon sequestration, *Int. J. Remote Sens.*, 30, 1479-1492,
656 <https://doi.org/10.1080/01431160802541549>, 2009.

657 John, J. G., Stock, C. A., and Dunne, J. P.: A more productive, but different, ocean after mitigation, *Geophys.*
658 *Res. Lett.*, 42, 9836-9845, <https://doi.org/10.1002/2015GL066160>, 2015.

659 Kanakidou, M., Seinfeld, J. H., Pandis, S. N., Barnes, I., Dentener, F. J., Facchini, M. C., Van Dingenen, R.,
660 Ervens, B., Nenes, A., Nielsen, C. J., Swietlicki, E., Putaud, J. P., Balkanski, Y., Fuzzi, S., Horth, J., Moortgat,
661 G. K., Winterhalter, R., Myhre, C. E. L., Tsigaridis, K., Vignati, E., Stephanou, E. G., and Wilson, J.: Organic
662 aerosol and global climate modelling: a review, *Atmos. Chem. Phys.*, 5, 1053-1123,
663 <https://doi.org/10.5194/acp-5-1053-2005>, 2005.

664 Kang, M., Fu, P., Kawamura, K., Yang, F., Zhang, H., Zang, Z., Ren, H., Ren, L., Zhao, Y., Sun, Y., and Wang,
665 Z.: Characterization of biogenic primary and secondary organic aerosols in the marine atmosphere over the East
666 China Sea, *Atmos. Chem. Phys.*, 18, 13947-13967, <https://doi.org/10.5194/acp-18-13947-2018>, 2018.

667 Kang, M., Guo, H., Wang, P., Fu, P., Ying, Q., Liu, H., Zhao, Y., and Zhang, H.: Characterization and source
668 apportionment of marine aerosols over the East China Sea, *Sci. Total Environ.*, 651, 2679-2688,
669 <https://doi.org/10.1016/j.scitotenv.2018.10.174>, 2019.

670 Kawamura, K., Hoque, M. M. M., Bates, T. S., and Quinn, P. K.: Molecular distributions and isotopic
671 compositions of organic aerosols over the western North Atlantic: Dicarboxylic acids, related compounds,
672 sugars, and secondary organic aerosol tracers, *Org. Geochem.*, 113, 229-238,
673 <https://doi.org/10.1016/j.orggeochem.2017.08.007>, 2017.

674 Kleindienst, T. E., Jaoui, M., Lewandowski, M., Offenberg, J. H., Lewis, C. W., Bhave, P. V., and Edney, E. O.:
675 Estimates of the contributions of biogenic and anthropogenic hydrocarbons to secondary organic aerosol at a
676 southeastern US location, *Atmos. Environ.*, 41, 8288-8300, <https://doi.org/10.1016/j.atmosenv.2007.06.045>,
677 2007.

678 Lauvset, S. K., Tjiputra, J., and Muri, H.: Climate engineering and the ocean: effects on biogeochemistry and

679 primary production, *Biogeosciences*, 14, 5675-5691, <https://doi.org/10.5194/bg-14-5675-2017>, 2017.

680 Lewandowski, M., Piletic, I. R., Kleindienst, T. E., Offenberg, J. H., Beaver, M. R., Jaoui, M., Docherty, K. S.,
681 and Edney, E. O.: Secondary organic aerosol characterisation at field sites across the United States during the
682 spring-summer period, *Int. J. Environ. Anal. Chem.*, 93, 1084-1103,
683 <https://doi.org/10.1080/03067319.2013.803545>, 2013.

684 Li, L., Tang, P., Nakao, S., Kacarab, M., and Cocker, D. R.: Novel approach for evaluating secondary organic
685 aerosol from aromatic hydrocarbons: unified method for predicting aerosol composition and formation, *Environ.*
686 *Sci. Technol.*, 50, 6249-6256, <https://doi.org/10.1021/acs.est.5b05778>, 2016.

687 Li, M., Zhang, Q., Streets, D. G., He, K. B., Cheng, Y. F., Emmons, L. K., Huo, H., Kang, S. C., Lu, Z., Shao,
688 M., Su, H., Yu, X., and Zhang, Y.: Mapping Asian anthropogenic emissions of non-methane volatile organic
689 compounds to multiple chemical mechanisms, *Atmos. Chem. Phys.*, 14, 5617-5638, 2014.

690 Li, R., Wang, Z., Cui, L., Fu, H., Zhang, L., Kong, L., Chen, W., and Chen, J.: Air pollution characteristics in
691 China during 2015–2016: Spatiotemporal variations and key meteorological factors, *Sci. Total Environ.*, 648,
692 902-915, 2019.

693 Meskhidze, N. and Nenes, A.: Phytoplankton and cloudiness in the Southern Ocean, *Science*, 314, 1419-1423,
694 <https://doi.org/10.1126/science.1131779>, 2006.

695 Mochida, M., Kawamura, K., Fu, P., and Takemura, T.: Seasonal variation of levoglucosan in aerosols over the
696 western North Pacific and its assessment as a biomass-burning tracer, *Atmos. Environ.*, 44, 3511-3518,
697 <https://doi.org/10.1016/j.atmosenv.2010.06.017>, 2010.

698 Murphy, D. M., Chow, J. C., Leibensperger, E. M., Malm, W. C., Pitchford, M., Schichtel, B. A., Watson, J. G.,
699 and White, W. H.: Decreases in elemental carbon and fine particle mass in the United States, *Atmos. Chem.*
700 *Phys.*, 11, 4679-4686, <https://doi.org/10.5194/acp-11-4679-2011>, 2011.

701 Nichols, M. A.: Spatial and temporal variability of marine primary organic aerosols over the global oceans: a
702 review, University of Maryland College Park, 2016.

703 Peñuelas, J. and Staudt, M.: BVOCs and global change, *Trends Plant Sci.*, 15, 133-144,
704 <https://doi.org/10.1016/j.tplants.2009.12.005>, 2010.

705 Rinne, H. J. I., Guenther, A. B., Greenberg, J. P., and Harley, P. C.: Isoprene and monoterpene fluxes measured
706 above Amazonian rainforest and their dependence on light and temperature, *Atmos. Environ.*, 36, 2421-2426,
707 [https://doi.org/10.1016/S1352-2310\(01\)00523-4](https://doi.org/10.1016/S1352-2310(01)00523-4), 2002.

708 Running, S. W.: Is global warming causing more, larger wildfires? *Science*, 313, 927-928,
709 <https://doi.org/10.1126/science.1130370>, 2006.

710 Sharma, S., Lavoué, D., Cachier, H., Barrie, L. A., and Gong, S. L.: Long-term trends of the black carbon
711 concentrations in the Canadian Arctic, *J. Geophys. Res.-Atmos.*, 109, D15203,
712 <https://doi:10.1029/2003JD004331>, 2004.

713 Shen, R., Ding, X., He, Q., Cong, Z., and Wang, X.: Seasonal variation of secondary organic aerosol tracers in
714 Central Tibetan Plateau, *Atmos. Chem. Phys.*, 15, 8781-8793, 2015.

715 Surratt, J. D., Chan, A. W. H., Eddingsaas, N. C., Chan, M., Loza, C. L., Kwan, A. J., Hersey, S. P., Flagan, R.
716 C., Wennberg, P. O., and Seinfeld, J. H.: Reactive intermediates revealed in secondary organic aerosol
717 formation from isoprene, *Proc. Natl. Acad. Sci. U.S.A.*, 107, 6640-6645,
718 <https://doi.org/10.1073/pnas.0911114107>, 2010.

719 Tarvainen, V., Hakola, H., Hellén, H., Bäck, J., Hari, P., and Kulmala, M.: Temperature and light dependence of
720 the VOC emissions of Scots pine, *Atmos. Chem. Phys.*, 5, 989-998, 2005.

721 van der Werf, G. R., Randerson, J. T., Giglio, L., Collatz, G. J., Kasibhatla, P. S., and Arellano Jr, A. F.:
722 Interannual variability in global biomass burning emissions from 1997 to 2004, *Atmos. Chem. Phys.*, 6,
723 3423-3441, 2006.

724 Wang, F., Guo, Z., Lin, T., Hu, L., Chen, Y., and Zhu, Y.: Characterization of carbonaceous aerosols over the
725 East China Sea: The impact of the East Asian continental outflow, *Atmos. Environ.*, 110, 163-173,
726 <https://doi.org/10.1016/j.atmosenv.2015.03.059>, 2015.

727 Warneke, C., Froyd, K. D., Brioude, J., Bahreini, R., Brock, C. A., Cozic, J., de Gouw, J. A., Fahey, D. W.,
728 Ferrare, R., Holloway, J. S., Middlebrook, A. M., Miller, L., Montzka, S., Schwarz, J. P., Sodemann, H.,
729 Spackman, J. R., and Stohl, A.: An important contribution to springtime Arctic aerosol from biomass burning in
730 Russia, *Geophys. Res. Lett.*, 37, L01801, <https://doi.org/10.1029/2009GL041816>, 2010.

731 Yang, F., Gu, Z., Feng, J., Liu, X., and Yao, X.: Biogenic and anthropogenic sources of oxalate in PM_{2.5} in a
732 mega city, Shanghai, *Atmos. Res.*, 138, 356-363, <https://doi.org/10.1016/j.atmosres.2013.12.006>, 2014.

733 Yang, F., Kawamura, K., Chen, J., Ho, K., Lee, S., Gao, Y., Cui, L., Wang, T., and Fu, P.: Anthropogenic and
734 biogenic organic compounds in summertime fine aerosols (PM_{2.5}) in Beijing, China, *Atmos. Environ.*, 124,
735 166-175, 2016.

736 Yao, X., Xu, X., Sabaliauskas, K., and Fang, M.: Comment on “Atmospheric Particulate Matter Pollution during
737 the 2008 Beijing Olympics”, *Environ. Sci. Technol.*, 43, 7589, <https://doi.org/10.1021/es902276p>, 2009.

738 Zhang, H., Surratt, J. D., Lin, Y. H., Bapat, J., and Kamens, R. M.: Effect of relative humidity on SOA
739 formation from isoprene/NO photooxidation: enhancement of 2-methylglyceric acid and its corresponding
740 oligoesters under dry conditions, *Atmos. Chem. Phys.*, 11, 6411-6424,
741 <https://doi.org/10.5194/acp-11-6411-2011>, 2011.

742 Zhang, Q., He, K., and Huo, H.: Policy: cleaning China's air, *Nature*, 484, 161-162, 2012.

743 Zhang, Y., Yang, X., Brown, R., Yang, L., Morawska, L., Ristovski, Z., Fu, Q., and Huang, C.: Shipping
744 emissions and their impacts on air quality in China, *Sci. Total Environ.*, 581-582, 186-198,
745 <https://doi.org/10.1016/j.scitotenv.2016.12.098>, 2017.

746 Zhang, Z., Zhang, Y., Wang, X., Lü, S., Huang, Z., Huang, X., Yang, W., Wang, Y., and Zhang, Q.:
747 Spatiotemporal patterns and source implications of aromatic hydrocarbons at six rural sites across China's
748 developed coastal regions, *J. Geophys. Res.-Atmos.*, 121, 6669-6687, <https://doi.org/10.1002/2016JD025115>,
749 2016.

750 Zhu, C., Kawamura, K., and Kunwar, B.: Effect of biomass burning over the western North Pacific Rim:
751 wintertime maxima of anhydrosugars in ambient aerosols from Okinawa, *Atmos. Chem. Phys.*, 15, 1959-1973,
752 <https://doi.org/10.5194/acp-15-1959-2015>, 2015.

753 Zhu, C., Kawamura, K., Fukuda, Y., Mochida, M., and Iwamoto, Y.: Fungal spores overwhelm biogenic organic
754 aerosols in a midlatitudinal forest, *Atmos. Chem. Phys.*, 16, 7497-7506, 2016a.

755 Zhu, C., Kawamura, K., and Fu, P.: Seasonal variations of biogenic secondary organic aerosol tracers in Cape
756 Hedo, Okinawa, *Atmos. Environ.*, 130, 113-119, <https://doi.org/10.1016/j.atmosenv.2015.08.069>, 2016b.

757 Zhu, Y., Yang, L., Kawamura, K., Chen, J., Ono, K., Wang, X., Xue, L., and Wang, W.: Contributions and
758 source identification of biogenic and anthropogenic hydrocarbons to secondary organic aerosols at Mt. Tai in
759 2014, *Environ. Pollut.*, 220, 863-872, 2017.

760 Zhu, Y., Li, K., Shen, Y., Gao, Y., Liu, X., Yu, Y., Gao, H., and Yao, X.: New particle formation in the marine
761 atmosphere during seven cruise campaigns, *Atmos. Chem. Phys.*, 19, 89-113,
762 <https://doi.org/10.5194/acp-19-89-2019>, 2019.